Fall 12-2016

Early Miocene Quantitative Calcareous Nannofossil Biostratigraphy from the Tropical Atlantic

Waheed A. Albasrawi
University of Nebraska-Lincoln, basrawwa@gmail.com

Early Miocene Quantitative Calcareous Nannofossil Biostratigraphy from the Tropical Atlantic

by

Waheed A. Albasrawi

A THESIS

Presented to the Faculty of

The Graduate College at the University of Nebraska

In Partial Fulfillment of Requirements

For the Degree of Master of Science

Major: Earth and Atmospheric Sciences

Under the Supervision of Professor David K. Watkins

Lincoln, Nebraska

December, 2016

Early Miocene Quantitative Calcareous Nannofossil Biostratigraphy from the Tropical Atlantic

Waheed A. Albasrawi, M.S.

University of Nebraska, 2016

Advisor: David K. Watkins

Quantitative analysis for the Lower Miocene of Ocean Drilling Program Hole 959A from the West African margin was performed to document all the calcareous nannofossil biostratigraphic events present. Combined with data from previous investigations of the Lower Miocene from the tropical Atlantic, this research identifies and tests the viability of markers used in current zonation scheme, identifies alternative markers for age boundaries, and examine statistically the most probable order of event in the Lower Miocene using the Ranking and Scaling method (RASC).

The examination of Hole 959A was performed on a 112 samples. Seven additional sites that collectively span the lower Miocene are used for the quantitative biostratigraphic analysis. These sites include DSDP Site 563 in the north central Atlantic (Maiorano and Monechi, 1998), Holes 897C, 898A, and 900A on the Iberian Abyssal Plain (De Kaenel and Villa, 1996),

Holes 960C and 960A on the Ivory Coast margin (Shafik et al., 1998), and DSDP Site 558 in the North central Atlantic (Parker et al., 1984).

In Hole 959A, all major zones and subzonal boundaries from CN1 to CN4 were identified, except for the boundary between Subzones CN1a and CN1b, using primary and secondary markers from Okada and Bukry (1980) zonation. All age boundaries were identified or closely estimated using the proper calcareous nannoplankton markers from the Chattian to Langhian stages.

The resultant list of events extracted from Hole 959A along with events from other seven sites were biostratigraphically examined in RASC. The well threshold is the only control parameter that was changed in order to select the appropriate control parameter. A well threshold of 4 was selected resulting in 22 events in the optimum sequence with 13 of which had a low standard deviation.

ACKNOWLEDGEMENTS

I would like to express my sincere appreciation to Dr. David Watkins, my advisor, for all the support during my master's program. He provided me with an excellent training in calcareous nannofossil biostratigraphy. Dr. Watkins was always there when I needed him to answer my questions and guide me throughout my project and for that I am forever grateful.

I would like also to thank the Earth and Atmospheric Sciences Department at UNL and my committee members Dr. David Harwood and Dr. Sherilyn Fritz for their insightful comments. I also would like to thank my nannofossil lab colleagues for their assistance, and special thanks goes to Shamar Chin for her continuous help. Finally, I thank Saudi Aramco for their sponsorship during my program.

Special thanks goes to my parents, wife and lovely daughter for their great support. This was not going to be possible without your support and for that I dedicate this degree to you all.

TABLE OF CONTENTS

List of Tables, Figures, Plates, and Appendix:

Figures:

Tables:

Plates:

Appendix:

Chapter 1 - Introduction

Documenting the occurrence of various biogeological events is one of the central goals of biostratigraphic studies. In geology, events found in different rock sequences can be linked together using the 'Law of Faunal Succession' and fossil correlation. Documenting events help also in understanding the most probable sequence of events in each stratigraphic unit and the evolution of a sedimentary sequence. In order to achieve these goals, a statistical analysis is performed on a set of events in the Lower Miocene, based on a detailed quantitative analysis of microfossils. These types of studies are fundamental for evaluating the reliability of the classic FO (First Occurrence) or LO (Last Occurrence) datums (Fornaciari and Rio, 1996). This study quantitatively documents the distribution of all the species encountered in the Lower Miocene section of Ocean Drilling Program (ODP) Leg 159, Hole 959A (Figure 1) to investigate the reliability of marker species and the biostratigraphic usefulness of secondary species. This will improve biostratigraphic resolution and precision in the application of Miocene calcareous nannoplankton biostratigraphy. Statistical analysis of different Lower Miocene sections using the Ranking and Scaling (RASC) method is adopted to define mapable biostratigraphic zones across the Lower Miocene in order to expand the existing quantitative database used to interpret the character and reliability of events in different geographic regions.

Although different ODP, IODP, and DSDP sites targeted the Miocene, only a few have focused on the Lower Miocene. Most studied sites were either barren of calcareous nannofossils or interrupted by hiatuses. For example, in ODP Leg 138 (Raffi and Flores, 1995), none of the sites penetrated any section below the CN3 Zone. Also, ODP Leg 198,

Site 1208 (Bown, 2005) had a short and condensed lower Miocene section with three major disconformities. ODP Leg, 159Hole 959A is one of the few sites that has a complete lower Miocene section represented by more than 133 meters of Lower Miocene sediments.

It has been generally accepted that the Lower Miocene starts from the boundary between Chattian-Aquitanian stages and continues up to the boundary between the Burdigalian-Langhian stages, spanning from 23.03 to 15.97 Ma, according to the latest geologic timescale (Gradstein et al., 2012).

Criteria for using calcareous nannofossils to approximate the Oligocene-Miocene boundary have changed over time. According to the standard Miocene zonation by Martini (1971) (Appendix 1) the boundary was placed within the base of Zone NN1 and associated with the last occurrence of *Helicosphaera truncata*. The Okada and Bukry (1980) zonation scheme (1980) (Appendix 2), defined the Paleogene (CP19b)/Neogene (CN1) boundary by the last occurrence of *Dictyococcytes bisecta*. Later, the beginning of the Neogene was modified in the geological time scale to 23.03 Ma (Gradstein et al., 2012), so that the Paleogene/Neogene boundary is placed in the uppermost part of CN1a. Different marker taxa have been used to define the upper part of the Oligocene: LO of *Helicosphaera recta*, which extends well into the Miocene (Rio et al., 1990), as well as the LO of *Sphenolithus ciperoensis,* which is noted over a million-years prior to the actual Oligocene-Miocene boundary (Raffi et al., 2006). According to Steininger et al. (1997) in their paper of the Aquitanian Global boundary Stratotype Section and Point (GSSP), *Sphenolithus ciperoensis*, *Sphenolithus delphix*, and *Sphenolithus capricorntus* are the main calcareous nannoplankton species associated with the Chattian-Aquitanian

stage boundary: The FO of *Sphenolithus ciperoensis* occurs within 21 meters below the boundary; The FO of *Sphenolithus delphix* occurs within 12 meters below the boundary; The FO and LO of *Sphenolithus capricorntus* occurs within 1 meter above the boundary; And the LO of *Sphenolithus delphix* occurs within 4 meters above the boundary. For the Aquitanian GSSP, microfossil reworking prevents the use of Last Occurrence datums, which have proven useful in other localities such as the LOs of *Zygrhablithus bijugatus* and *Reticulofenstra bisecta*. Other microfossil groups are used to identify the boundary such as: planktonic foraminifera, benthic foraminifera, and dinoflagellate cysts. The interpreted data of the correlation of biostratigraphic datums using the magnetobiochronologic scale of Berggren et al., (1995) show that the Chattian-Aquitanian boundary is placed between Chron C6Cn.2r and Chron C6Cn.2n.

The Aquitanian/Burdigalian stage boundary has not been ratified formally as of yet. Many sites have been proposed as the GSSP of the boundary but no site has been agreed upon as a stratotype. According to Gradstein et al., (2012) offshore sites have been nominated to identify a GSSP for the Burdigalian GSSP boundary including, ODP sites 1090, 1264/1265 and sites drilled on IODP leg 321 and 322. Only a few holes from this list of proposed sites comprise the Lower Miocene section. At site 1090, most markers of the Lower Miocene (NN1-NN3) were absent or scarce in abundance (Marino and Flores, 2002). Proposed boundary markers are absent in Site 1264, however they are present in Site 1265 with poor preservation, based on the data provided by the Shipboard Scientific Party (2004) for sites 1264 and 1265. Hole 959A (this study) has a potential to be considered for a valid GSSP for the boundary between the Aquitanian/Burdigalian stages. The definition of that boundary has four possible options, two of which are calcareous

nannofossil species: the FO of *Helicosphaera ampliaperta* at 20.43 Ma (Fornaciari and Rio, 1996), and the FO of *Sphenolithus belemnos* dated at 19.03 Ma (Haq et al., 1987). Other possibilities are the LO of planktonic foraminifer *Paragloborotalia kugleri* dated at 21.12 Ma (Berggren et al., 1995) and the top of Chron C6An dated at 20.04 Ma (Berggren et al., 1995) In Hole 959A, two of the four possibilities for the base Burdigalian boundary are present, which are the FO of *Helicosphaera ampliaperta* and the FO of *Sphenolithus belemnos*.

The boundary between the Aquitanian and the Burdigalian stages in the Astronomically Tuned Neogene Time Scale 2004 (ATNTS2004) was provisionally placed to coincide with the FO of *Helicosphaera ampliaperta*, which has an astronomically tuned age at 20.43 Ma according to the latest geological timescale (Gradstein et al., 2012).

The aim of this present study is to use the detailed analysis done on Hole 959A to increase the resolution of Early Miocene calcareous nannoplankton biostratigraphic zones. Also, examining the use and presence of primary and secondary species markers events of all the boundaries in the Lower Miocene. This includes examining the closest markers to be used for the Aquitanian and Burdigalian stages boundary as presented above. Finally, compare the results obtained from Hole 959A with other sites, that span the early Miocene, in a statistical quantitative analysis using RASC to interpret the optimum order of bioevents in the Early Miocene.

Chapter 2 - Materials and Methods

A total of 112 samples from the lower Miocene of Hole 959A were analyzed (barren

samples were omitted later in the composite analysis sheet) with 30-100 cm spacing in distance and an average of 105 ka spacing in time between samples. Biostratigraphic data were collected from prepared slides by light microscope examination. Smear slides were prepared using a 'double suspension' method. This method involves removing a small amount of sediment from a fresh, large surface and then suspending it in water on a cover slip. The sediment is then smeared on the slide. Once dried, then sediment is re-suspended in water to form slurry and smeared again to ensure proper spreading of the calcareous nannofossils assemblages on the slide and also prevent any improper size or shape fractionation of the fecal pellets on the slide. Watkins and Bergen (2003) confirmed statistically that this method show no distributional bias due to nannofossil size or shape (confidence interval > 99.99%). Counts of calcareous nannofossil assemblages were made using an Olympus BX-51 microscope at 1000X magnification and species images were taken using an Olympus DP71 camera. The cascading counting technique developed by Styzen (1997) was used to collect assemblage data for all sample sets for a total of 30 fields-of-view (FOV) and then continuing for the remainder of the traverse, and two additional traverses were made to locate especially rare species. The PAST (PAleontological STatistics) v. 3.04 (Hammer et al., 2001) and OriginPro v. 7.5 software packages were used for statistical analysis and graphic representation.

The abundance of nannofossils as a sedimentary component and the preservation of the nannofossil assemblages are designated following the method in Watkins et al. (1998). The abundance of nannofossils as a component of the sediment is defined as follows: A = >50% of sediment by volume; C = 15%-50% of sediment by volume; F = 1%-15% of sediment by volume; and R = <1% of sediment by volume. An average state

of preservation was assigned to each sample according to the following criteria: G = good, most specimens exhibit little or no secondary alteration; M = moderate, specimens exhibit the effects of secondary alteration from etching and/or overgrowth (identification of species not impaired); P = poor, specimens exhibit profound effects of secondary alteration from etching and/or overgrowth (identification of species impaired but possible in some cases).

The Okada and Bukry (1980) zonation scheme is used as the standard zonation scheme for this study. It was formulated from low latitude sites and thus should work well for this study. The zonation of Martini (1971) was not used in this study but its applicability is commented on below.

Hole 959A was studied previously by Shafik et al., (1998) as part of a preliminary analysis of six holes from ODP Leg 159 (Holes 959A, 959B, 960A, 960C, 961A, and 962B). All of these holes targeted the Neogene (Miocene, Pliocene, Pleistocene) with Hole 959A being the thickest Lower Miocene section which was apparently uninterrupted by hiatuses. The study done by Shafik et al., (1998) correlated the biozones and hiatuses with the sea level curve by Haq et al. (1987).

For the interval of Hole 959A examined here, there are neither magnetostratigraphic data nor any other type of temporal control, such as: foraminiferal biostratigraphic analysis. Magnetic data acquisition was performed for Hole 959A, but signals were weak and therefore no magnetostratigraphic data is valid for this hole. (Allerton, 1998).

Data from seven additional holes that collectively span the lower Miocene were chosen for quantitative biostratigraphic analysis (Figure 1). These sites include, DSDP

Site 563 in the north central Atlantic Ocean (Maiorano and Monechi, 1998), Holes 897 C, 898 A, and 900 A on the Iberian Abyssal Plain (De Kaenel and Villa, 1996), Holes 960C and 960A on the Ivory coast margin (Shafik et al., 1998), and DSDP Site 558 in the North central Atlantic Ocean (Parker et al., 1985). Only DSDP Site 563 (Maiorano and Monechi, 1998) has a quantitative data, the remaining sites present qualitative analysis data. Sites/Holes were selected based on quality of biostratigraphic data, and availability. Sites analyzed prior to the 1980's were omitted to allow for more up-to-date analyses. It was important to incorporate record from as many sites as possible that spanned the most complete Lower Miocene, in order to observe all the possible bioevents.

Chapter 3 - Ranking and Scaling Method

Gradstein and Agterberg (1982) introduced the original concept of the Ranking and Scaling method (RASC) in a Cenozoic foraminiferal study in offshore wells along the northwestern Atlantic margin (Bowman, 2011). Further modifications, detailed work, and application were later introduced (Agterberg and Gradstein, 1997a, 1997b, 1999; Agterberg et al., 1998; and Gradstein and Agterberg, 1998). The RASC is a statistical, probabilistic technique used to compute the optimum sequence of events. The optimum sequence is evaluated statistically based on the cross-over frequencies of bioevents. Cross-over is when a bioevent occurs in reverse order in another well. For example, if event A occurs above event B in one site and Event B occurs above event A in a different site, then this is considered as a cross-over of events. The optimum sequence should include the ranking of events with the minimum number of cross-over. The analysis produces a list of events with a calculated standard deviation. Events with lower standard deviation than the average standard deviation of the optimum sequence are considered to

be more reliable events than those with higher standard deviations.

The RASC technique consists of two steps that help in producing the most probable sequence of events. The first step is ranking; that is to rank all the bioevents in order of their occurrence compared to each other. The second step is scaling; which involves a statistical determination of the relative spacing of bioevents. The ranking step compares the occurrences of an event relative to the other events. For example: If an event occurs 4 out of 5 times below another event, then it is considered to be the stratigraphically lower event. And if both events co-occur with an equal number then their stratigraphic order is indeterminate, but assumed to be closely related temporally. The full sequence is created when all events are ranked in relation to each other. The scaling step determines the relative distance stratigraphically between the ranked events. The relative distance is affected by the ranking of the events and the number of wells in which the two bioevents co-occur (Gradstein et al., 1990). If an event occur frequently above another event (lower number of cross-overs) then the distance between the two events is great. Conversely, if both events co-occur with a similar number of cross-overs, then the separation distance is relatively small, because we cannot determine which event is stratigraphically higher than the other. The cross-over between events could be *in situ* or in other cases could be an error due to reworking, caving, digenesis, misidentification and/or basic sampling errors (Agterberg and Gradstein, 1999).

Chapter 4 – Results

4.1- Hole 959A analysis

The Lower Miocene calcareous nannofossil assemblages recovered in Hole 959A are presented in detail on the distribution chart (Appendix 3). Important species are

illustrated in Plates 1 through 5. A total of 58 formal species were identified in the lower Miocene section including multiple *Discoaster*, *Helicosphaera*, and *Sphenolithus* species. Species of the genus *Reticulofenstra* and *Dictyococcytes* were placed into size categories as proposed by Young (1997). Nannofossils are mostly abundant throughout the assemblages, except for few samples in the lowermost section in which the abundance is moderately to low. Nannofossils are moderately to well-preserved throughout the lower Miocene sequence. Barren intervals were encountered near the Oligocene-Miocene boundary. Most of the cores (cores 35 to 30) were interrupted by barren sections or poor to moderate preservation, and moderate to low counts of species compared to the upper cores. As stated above, the Okada and Bukry (1980) zonation scheme, which was prepared on a set of low latitude sites, is used to interpret the biozones of Hole 959A, which is located on the "transform belt", about 3° north of the Equator (Figure 1).

The Okada and Bukry (1980) zonation defined the CP19b/CN1 boundary based on the last occurrence of *Dicctyoccocytes bisectus* and/or *Sphenolithus ciperoensis,* but neither of these species was encountered in this study. Given that, an alternative marker was used for the boundary between Oligocene-Miocene at the LO of *Sphenolithus delphix* based on the astrobichronology data by Raffi et al., (2006) and Steininger et al. (1997) in the Aquitanian GSSP.

The subzonal CN1a/b boundary could not be differentiated reliably due to the absence of *Cyclicargolithus abisectus;* the end of the acme of *Cyclicargolithus abisectus* is the criterion for identifying the base of Subzone CN1b. The Subzone CN1b/c boundary was identified by the first occurrence of *Orthorhabdus serratus* in sample 29-6, 60-61,

which is the secondary/alternative marker used for this subzone following Bukry (1973) and Olafsson (1989). The primary marker for Subzone CN1 as defined by Okada and Bukry (1980) is the FO of *Discoaster druggii*; however its rare occurrence in the section rendered it unreliable. The base of Zone CN2 was picked based on the first occurrence of *Sphenolithus belemnos* in sample 28-5, 100-101. Zone CN3 is identified by the first occurrence of *Sphenolithus heteromorphus* at the core break in sample 26CC. Finally, the CN3/CN4 Zonal boundary is identified based on the last occurrence of *Helicosphaera ampliaperta*, which last occurred in sample 21-1, 48-49. Appendix 4 provide a summary for age and boundary markers for the Lower Miocene section in Hole 959A.

A summary of bioevents from Hole 959A are listed in Table 1. The events were extracted from the distribution chart of the well and they included multiple types of datums; First Occurrence datums (FO), Last Occurrence datum (LO), First Common Occurrence datum (FCO), Last Common Occurrence datum (LCO), Beginning of an Acme (F-Acme), and End of an Acme (L-Acme).

4.2 – Ranking and Scaling Analysis

There are 4 control parameters for RASC in PAST; Well threshold, Pair threshold, Scaling threshold, and Tolerance. Only the well threshold parameter was examined in this study due to the intention of producing a more global sequence that works on multiple wells in not necessarily examine the pairing relationship between events. In order to determine the best control parameters for our study, we tried multiple RASC runs with different “well threshold” values. This value indicates the minimum number of wells in which a certain bioevent must occur to be included in the analysis (‘k’ value). There is an

inverse relationship between the 'k value' and the number of events used in the analysis. The higher the 'k' value, the lower the number of events because the cutoff requirement is higher and may not occur in all sites. For example, if the 'k' value was "5", then the event has to occur in 5 wells to be considered in the ranked sequence. As the value of 'k' increases fewer events are produced, because of the higher possibility that such events may not occur in more than 5 wells. In general, there are no exact criteria for determining the optimal value of 'k', but rather it depends more on the balance between the higher numbers of events produced with the number of events with lowest cross over. In our RASC analyses we used different runs with different 'k' values (from 1 to 8; Table 2). We subjectively selected the 'k' value based on percentage of the highly probable events compared to the overall number of events (Figure 2). The well threshold selected for this study is 'k'= 4.

Chapter 5 – Discussion

5.1 Hole 959A

No calcareous nannoplankton events define the Oligocene/Miocene boundary exactly, however, two species events occur very close to the boundary. The first event used to approximate the Oligocene/Miocene boundary is the LO of *Sphenolithus delphix*, which goes extinct according to Raffi et al., (2006) around 23.06 Ma and according to the latest geological time scale around 23.11 Ma. The astronomically tuned age for the last occurrence of *Sphenolithus delphix* is a little over 30 ka younger than the boundary, which apparently is the closest event to the boundary. The second event is the FO of *Sphenolithus capricorntus*, which is defined at an astronomically tuned age in the latest geological time scale at 22.97 Ma and at the base of C6Cn.2n.5 chron, which is older than

the Oligocene/Miocene boundary by also a little over 30 ka. In Hole 959A, another event was used in the process of defining the Oligocene/Miocene boundary. The base of *Sphenolithus disbelemnos*, which is dated around 22.76 Ma based on Raffi (2006), is around 300 ka younger than the boundary. *Sphenolithus capricorntus* was not encountered in Hole 959A but the last occurrence of *Sphenolithus delphix* was encountered at 322.47 mbsf. The first occurrence of *Sphenolithus disbelemnos* occurs at 322.20 mbsf and so the boundary between the Oligocene/Miocene must occur in the 27 cm gap in between the two samples. Unfortunately, the material acquired from that gap is barren of calcareous nannoplankton. As a result, the Miocene/Oligocene boundary is defined in the barren interval between the LO of *S. delphix* and the FO of *S. disbelemnos*.

The subzonal boundary CN1a/b is defined at the end of the acme of *Cyclicargolithus abisectus* (Okada and Bukry, 1980). *Cyclicargolithus abisectus* is very similar to the species *Cyclicargolithus floridanus* and they can be distinguished only by size. Olafsson (1989) noted, "It is virtually impossible to distinguish *C. floridanus* from *Cyclicargolithus abisectus* by the original descriptions of the two species. They both show the same optical behavior and their sizes overlap considerably". Although the size differentiation method between *C. abisectus* and *C. floridanus* is arbitrary, it is of a biostratigraphical importance and so in this study we used a cut-off size of >10 μm to differentiate the two species, following Fornaciari et al. (1990). No *Cyclicargolithus* species larger than 10 μm were encountered in the section and therefore *Cyclicargolithus abisectus* does not occur in Hole 959A. The end of the acme of *Cyclicargolithus abisectus* only defines Zone CN1a/b according to Okada and Bukry (1980) and in this study, the zonal boundary was not identified.

The first occurrence of primary marker *Discoaster druggii* and/or FO of the secondary marker *Orthorhabdus serratus* define the base of Subzone CN1c according to Bukry (1973) and Olafsson (1989). *Discoaster druggii* is not common in Hole 959A and only occurs in 3 samples in low abundance. *Discoaster druggii* has been separated in this section into two species: *Discoaster druggii* and *Discoaster* sp. *cf D. druggii*. The division of this species is based on size alone. *Discoaster druggii* (*sensu stricto*) is defined with a size greater than 15 μm and tapered arms that terminate in small bifurcations (following Rio et al., 1990). A morphologically similar form (*Discoaster* sp. *cf. D. druggii*) occurs in other samples, but differs by its smaller size (substantially <15 μm). The low abundance/occurrence of *Discoaster druggii* makes it an unreliable marker for this zone. Therefore, the FO of *Orthorhabdus serratus* was used in Hole 959A as the key marker for the base of Subzone CN1c.

The boundary between the Aquitanian and the Burdigalian stages, (ca. 20.44Ma, according to the latest update by the International Commission on Stratigraphy (ICS) and Gradstein et al., 2012) has not been ratified as of yet. Two possible nannofossil events suggested by Gradstein et al. (2012) as markers for the boundary are the FO of *Sphenolithus belemnos* and the FO of *Helicosphaera ampliaperta*. *Sphenolithus belemnos* is used as zonal marker for Zone CN2 according to Okada and Bukry (1980) and its astronomically tuned age, according to the latest time scale (2012), is dated around 19.03 Ma, which is about 1 Ma older than the assigned ATNTS2012 age for the Aquitanian/Burdigalian boundary. In Hole 959A, *Helicosphaera ampliaperta* occurs in sample 28CC prior to the FO of *Sphenolithus belemnos* in sample 28-2,10-11. Both events are 7.48 m apart from each other. The boundary between Aquitanian and the

Burdigalian stages in Hole 959A can be defined by the FO of *H. ampliaperta*, which is dated at 20.43 Ma according to the latest ATNTS2012 (Gradstein et al., 2012). The ICS is currently nominating the Burdigalian Stage to be near the FAD of the planktonic foraminifer *Globigerinoides altiaperturus* or near the top of magnetic polarity chronozone C6An.

Zone CN3 is defined by both the first occurrence of *S. heteromorphus* and the LO of T. *carinatus*. The FO of *S. heteromorphus* occurs in sample 26CC and the last occurrence of T. *carinatus* occurs in sample 26-2, 120-121. In Hole 959A, in the interval from sample 26CC to 25-6, 5-6, *S. heteromorphus* occurs and then afterward the continuous abundance increase, which is used here to define boundary between the CN2 and CN3 Zones. The LO of *T. carinatus* is used as a secondary marker for the base of CN3 Zone. It occurs very closely prior (~ 4.85 m) to the FCO of *S. heteromorphus* in Hole 959A.

Lastly, Zone CN4, which is defined by the last occurrence of *Helicosphaera ampliaperta* and/or end of the *Discoaster deflandrei* acme. In this study, the last occurrence of *Helicosphaera ampliaperta* is used to define the CN3/CN4 boundary because it marks a sharp boundary in the section. The end of the *Discoaster deflandrei* acme occurs lower, in sample 22-3, 48-49, than the last occurrence of *H. ampliaperta*, and is more difficult to pinpoint because of its gradual nature. The LO of *H. ampliaperta* is dated at 14.91 Ma, ATNTS2012, near the middle of Chron C5Br (Gradstein et al., 2012).

The boundary between the Burdigalian and the Langhian stages is commonly used to divide the lower and middle Miocene. The base of the Langhian is assigned an astronomically calibrated age of 15.97 Ma (Gradstein et al., 2012). Two criteria are used

to define the base of the Langhian: the FO of *Praeorbulina glomerosa* and the top of C5Cn chron (Gradstein et al., 2012). Further magnetostratigraphic and calcareous plankton studies have recommended the provisional placement of the Langhian GSSP to coincide with the top of C5Cn.1n, dated astronomically at 15.974 Ma in ATNTS2004 (Gradstein et al., 2012). The calcareous nannoplankton bioevent that approximates the magnetic reversal is the LCO of *H. ampliaperta*, which is considered as a reliable event in the Mediterranean region (Turco et al., 2011a). Another event that could be used as an approximation to the boundary is the first occurrence of *Discoaster signus*, which postdates the boundary by approximately 27 ka (has an astronomically calibrated age of 15.70 Ma (Gradstein et al., 2012)). In this study, *Discoaster signus* was not encountered in the analysis and *H ampliaperta* was continuous until its extinction with a varying abundance, which make it difficult to pick the LCO of *H. ampliaperta*. In this study the boundary between the Burdigalian and the Langhian was picked closer to the LCO of *Discoaster deflandrei*, which has an assigned C5Br chron and an assigned age of 15.80 Ma, ~ 17 ka younger than the boundary (Gradstein et al., 2012).

5.2 Age/Depth model

The Age/Depth model for Hole 959A (Figure 3) shows a linear relationship. The events used to plot the age/depth model are events with defined ages found in the latest geological time scale (Gradstein et al., 2012) and in Raffi et al. (2006), data found in Table 3a. Only one data point occurs on the offset of the line in the middle section, the *Discoaster druggii* value, which appears to be a bad value and could be attributed to the sporadic and rare nature of *D. druggii*. The calculated sediment accumulation rate from Figure 3 is 16.3 m/Ma, which is considered as a moderately high sediment accumulation

rate. Ages for other events have been interpolated using the equation of the linear line (best fit line) and then by solving for the age. Table 3b show the interpolated age ranges for the different events from Hole 959A, and similarly Table 4 show the ages extrapolated from the other wells used in this study based on each well's age/depth model. After plotting the age/depth value for each well and plotting the best fit line, the equation for the best-fit line was used to interpolate the age values for that well.

The age values of wells in Table 4 fall within a varied age range. For instance, the last occurrence of *Sphenolithus dissimilis* occur in Hole 897C at 22.615 Ma (the oldest age value) and the youngest age value occurs in Hole 960A around 16.787 Ma (the age values were extrapolated from the age/depth model of the data by De Kaenel et al., 1998 and Shafik et al., 1998, respectively). All other extrapolated values for LO of *S. dissimils* occurred in between these two values with an average of 18.890 Ma. In this study is assumed a constant sediment accumulation rate, which might not be the case in all the holes and therefore can explain the different age values. Other explanation could be due to misidentification of species, caving, reworking, or patchiness of occurrence. The resolution in the previous example is within 1 Ma. Other examples show a larger gap in extrapolated ages between different wells. Events with the most closely extrapolated ages, compared to those with wide age-extrapolated age ranges, can be used as a reasonable preliminary estimate of secondary events.

Plots of the abundance (species count) and richness (number of different species per sample) with depth for Hole 959A show certain characteristics for each zone. In Figures 4 and 5 Zone CN1 has fluctuating counts of species and also a fluctuating richness curves, generally in the lower side values of both. Zone CN2 show an increasing trend of

both count and richness. Zone CN3 and CN4 also show a decreasing trend of count and richness compared to that in CN2 Zone. Those curves could be interpreted and studied further to illustrate any environmental factors affecting the calcareous nannofossil abundances and richness.

5.3 The RASC Analysis

The correlation scheme based on the RASC generated optimum sequence increased biostratigraphic resolution, eliminated less reliable bioevents, and added key non-traditional bioevents. During RASC analysis, a comparison table of the number of events produced in relation to the well threshold value was used to determine which value of 'k' would be used (Table 2). A value of 4 was used as the threshold parameter for the minimum number of wells that a bioevent must occur in to be included in the optimum sequence. The RASC run with k=4 produced 22 total bioevents in the optimum sequence, 11 of which had standard deviations below the average. For comparison, the RASC run with k=5 produced 18 total bioevents in the optimum sequence, with 9 bioevents possessing standard deviations lower than the average. 'k' value of 4 produced the preferred optimum sequence because it contained the most bioevents while maintaining a reliable number of events with low cross over. Therefore k=4 results are the most useful optimum sequence in this study.

The average standard deviation produced by the final RASC run (k=4) was 0.143. Table 5 and Figure 6 show an illustration of the final optimum sequence, indicating the list of bioevents with their standard deviations and the number of wells in which each occurred.

5.2a – Events with Low standard deviation

By applying the RASC method, the optimum sequence produced 13 correlated events in wells with low cross-over frequencies and another 9 events with high standard deviation (High cross-over frequencies). A detailed description for the events with the low standard deviation is listed below:

LO *Sphenolithus delphix*:

As described above, this event is used to approximate the base of Lower Miocene. Agnini et al., (2014) stated that the LO of *Sphenolithus delphix* provides a distinct biohorizon occurring 30 kyr prior to the Oligocene/Miocene boundary. Rio et al. (1990) indicated that *S. delphix* often found associated with *S. capricorntus*. It is present only in 4 out of 8 wells, which is reasonable considering the difficulty associated with picking that event, especially when the preservation is poor and species are broken and/or overgrown. Most of the Oligocene-Miocene boundary sections used in this study either had low count or poorly preserved species, which could be attributed to the misidentification of this event.

FO *Orthorhabdus serratus*

As stated above, this event has been used as a secondary marker for the base of Subzonal boundary CN1c. Several sites have reported this event as rare and sporadic, such as DSDP Site 563 (Maiorano and Monechi, 1998). In Hole 959A, this event was easily identified and continuous from its first occurrence until the middle of Zone CN2 when it starts to have an intermittent occurrence with low counts. This event occurs in 7 out of 8 holes.

FO *Sphenolithus belemnos*

This event is usually associated with FO of *H. ampliaperta*. Both events are linked

and currently used to approximate the Aquiatanian/Burdigalian boundary. FO of *Sphenolithus belemnos* has an astronomically tuned age that is slightly younger than that of FO of *H. ampliaperta* by 1.4 Ma (Gradstein et al., 2012). The FOs of *H. ampliaperta* and *S. belemnos* are observed at the same level in Holes 898A and 900A (De Kaenel and Villa, 1996). In Hole 959A, *S. belemnos* postdated that of *H. ampliaperta* by 7.91 mbsf. This event occurs in 7 out of 8 holes.

LO *Triquetrorhabdulus carinatus*

This event is used in Martini (1971) zonation scheme to define the NN2-NN3 boundary, but according to Maiorano and Monechi (1998), it is generally unreliable marker event. However, many workers use the decrease in abundance of *T. carinatus* at the base of CN1c as a more reliable event (Rio et al., 1990a; Fornaciari et al., 1993; and Maiorano and Monechi 1998). De Kaenel and Villa (1996) documented the LO of *T. carinatus* just below the LO of *S. belemnos* at Sites 898 and 900. In Hole 959A, the *LO of T. carinatus* occur at the uppermost CN2 Zone; the LO of *S. belemnos* event predate the LO of *T. carinatus*. In Hole 959A, the decrease in abundance of *T. carinatus* occur in the middle of CN1a/b Subzone and almost the entire CN1c Subzone. In CN2 Zone, *T. carinatus* is sporadic in count but almost continuous until its last occurrence in sample 26-2, 120-121. This event occurs in all the holes used in the RASC study.

FO *Sphenolithus heteromorphus*

This event defines the base of Zone CN3. It has been observed in many sites that there is an overlap between *Sphenolithus heteromorphus* and *S. belemnos* such as Bukry (1972) at Site 140 in the Atlantic Ocean, Pujos (1985) in the equatorial Pacific, Maiorano and Monechi (2005) in Site 563, De Kaenel and Villa (1996) in sites 899-900 and

Takayama and Sato (1987) in the North Atlantic. Other workers did not recognize this overlap such as the analysis done by Olafsson (1989), in the equatorial Atlantic Ocean, Fornaciari et al. (1990) in the Indian Ocean, and Gartner (1992) in the North Atlantic Ocean. In Hole 959A, the overlap was encountered between *S. heteromorphus* and *S. belemnos*. This event seems to be one of the clearest events of the Lower Miocene, it occurs in all the holes used in the RASC study.

LO *Sphenolithus dissimilis*

This event occurs in the upper CN1c Subzone. It is usually associated with FO of *H. ampliaperta*. According to Marunteanu (1999), the *Discoaster druggii*-NN2 Zone can be subdivided into the *Sphenolithus dissmilis* (NN2a) and *Helicosphaera kamptneri* (NN2b) Subzone, on the basis of the first occurrence of *Helicosphaera ampliaperta*, which corresponds to the disappearance of *Sphenolithus dissimilis*. In Hole 959A, LO of *S. dissimilis* overlaps in a short range with the FO of *H. ampliaperta*. This event occurs in 7 out of 8 wells.

LO *Sphenolithus belemnos*

S. belemnos has a total range within Zone CN2. Its LO is associated with the lowest occurrence of *S. heteromorphous*. According to De Kaenel and Villa (1996), both events occurred close to each other but always separated by a short interval, as is the case at ODP Site 900. On the other hand, at DSDP Site 563 the LO of *S. belemnos* co-occurs with the lowest occurrence of S. *heteromorphous*. In Hole 959A, it is similar to Site 563 where both bioevents co-occur within a short range. This event occurs in 7 out of 8 holes.

FO *Discoaster petaliformis*

De Kaenel and Villa (1996) have associated the FO of *D. petaliformis* with FO of *D.*

exilis such as in Sites 898 and 899. In Hole 959A, *D. petaliformis* occurs in the middle-upper part of Zone CN3, while *D. exilis* occurred in the lowermost section of Zone CN3. Thus, the association between this event and FO *D. exilis* was not demonstrated in this section. This event has occurred in 4 out of 8 wells.

LO *Helicosphaera euphratis*

In Hole 959A, this event occur in the uppermost section of the CN3 Zone. De Kaenel and Villa (1996) separated *H. euphratis* based on size and stated that the LO of the larger form of H. euphratis (> 8 μm) is a useful biohorizon in the upper Zone NN2. This event occurs in 6 out of 8 wells.

FO *Discoaster exilis*

As stated above, this event has been associated with the FO of *D. petaliformis* which was not demonstrated in Hole 959A. This event occurs in 6 out of 8 holes.

LCO *Discoaster deflandrei*

Bukry (1973) suggested the *D. deflandrei* acme end and the LO of *H. ampliaperta* for defining CN3/CN4 boundary. Many biostratigraphy workers have associated a drop in abundance of *D. deflandrei* at the FO of *D. signus* such as Rio et al. (1990) in the Indian Ocean, Raffi and Flores (1995) in the eastern equatorial Pacific Ocean, and Miorano and Monechi (2005) in Site 563. In Hole 959A, the end of the *D. deflandrei* acme occurs at the upper part of CN3 Zone just before the LO of *H. ampliaperta*. This event was not associated with any presence of *D. signus*. This event occurs in 5 out of 8 wells. In other sections this event is used as an alternative for CN3/CN4 boundary when LO *H. ampliaperta* is not present (Maiorano and Monechi, 1998).

LO *Triquetrorhabdulus milowii*

This event is usually co-occur together with the LO of *H. ampliaperta*. This has occurred in the four sites from Leg 149 (De kaenel and Villa, 1996). In Hole 959A, both event occur very close to each other where the LO of *T. milowii* occur in the uppermost part of Zone CN3 in sample 21-3, 48-49, while the LO of *H. ampliaperta* occur in sample 21-1, 48-49. Overall, this event occurs in 7 out of 8 holes.

FCO *Discoaster variabilis*

In Hole 959A, the FCO of *D. variabilis* occurs in the lower section of Zone CN3; it precedes the LO of *T. milowii* by 37.05 mbsf. Prior studies did not report it as a reliable event. This event occurs in 4 out of 8 holes.

5.2b – Events with High standard deviation

The RASC analysis yielded 9 events with higher standard deviation than the average of 0.1389. The events are: FO of *Discoaster* sp. *cf. druggii*, FO of *Discoaster druggii*, LO of *Helicosphaera recta*, LO of *Sphenolithus conicus*, FO of *Helicosphaera ampliaperta*, FO of *Calcidiscus premacintyrei*, Acme end of *Coronocyclus nitescens*, FO of *Discoaster variabilis*, and LO of *Helicosphaera ampliaperta*.

Four of the consecutive events in the lowest Miocene section have high standard deviations (Figure 6); from the FO of *Discoaster* sp. *cf. D. druggii* until the LO of *Sphenolithus conicus*. Two of these events are considered as major events (primary or secondary markers) that are used in the Lower Miocene to pick subzonal boundaries in Zone CN1; *Discoaster druggii* is the primary marker for Subzone CN1C, and the LO of *Helicosphaera recta*, which was considered as a marker event for the upper Oligocene

(Rio et al., 1990). The high standard deviation value for these events could be attributed to the sporadic occurrence of *Discoaster druggii*.

Events associated with the species *Helicosphaera ampliaperta* are considered as major events used in the Okada and Bukry's (1980) zonation. The FO is used as a secondary marker for Zone CN2 and also, as stated above, a potential for the Burdigalian GSSP, while the LO is used as the primary marker for the base of Zone CN4. The FO of Helicosphaera *ampliaperta* occurs in 7 out of 8 holes, while the LO of *Helicosphaera ampliaperta* occurs in 6 out of 8 holes. Although both events occur in most of the holes used in this study, they seem to have a high cross-over frequency and therefore a high standard deviation.

Although it did not appear as a result in the RASC analysis, *Sphenolithus disbelemnos* proved useful in its biostratigraphical range, which is different than that of *Sphenolithus belemnos*. Most of the sites used in this study did not identify this species in its range chart. It may have been included in the analysis combined with the species *Sphenolithus belemnos* or *Sphenolithus exilis*. The *Sphenolithus disbelemnos* is named by Fornaciari & Rio (1996) and so this species should be missing from the analysis for any site done prior to 1996 or within a closer range. *Sphenolithus disbelemnos* has only been found in Hole 959A (this study), and in Maiorano and Monechi (1998) DSDP Site 563. Proper reanalysis of the data from the sites used in this study may indeed affect the RASC analysis, and might in turn suggest the *S. disbelemnos* as a valid correlational event.

Chapter 6 - Conclusions

Detailed quantitative analysis is established for the Lower Miocene of ODP Leg 159, Hole 959A. Multiple events are documented and compared with data from eight other

sites. The other sites were selected based on their completness of data, availability, ease of access, and the newest available data for lower Miocene. Based on the analyzed section, the boundary between the Oligocene and the Miocene is approximated based on the LO of calcareous nannofossil *S. delphix,* which is the closest identified datum to the base of Aquitanian stage in Hole 959A. The CN1a/b boundary marker was not picked due to the absence of *C. abisectus*. On the other hand, CN1c Subzone was picked based on the FO of *O. serratus* due to the unreliability of the primary marker of the zone *D. druggii*. The FO of *S. belemnos* was used to pick Zone CN2, while the FCO of *S. heterormorphus* was used to pick Zone CN3. Finally, base of Zone CN4 was picked based on the last occurrence of *H. ampliaperta*. The boundary between the Aquitanian and the Burdigalian is picked based on the FO of *H. ampliaperta,* which occurs prior to the FO of *S. belemnos* in Zone CN2. Interpolation of ages of events assuming linear sediment accumulation provides a reasonable preliminary age estimate of secondary events. The quantitative analysis was run using RASC in order to find the optimum sequence in which the data have a minimum cross-over of events. The generated optimum sequence, which consists of 22 events, 13 of which had a minimum standard deviation, matches the sequence of events in Hole 959A.

References:

Allerton, S., 1998. Paleomagnetic Results from Holes 959D and 960A, Côte D'ivoire-Ghana Transform Margin, *Proc. ODP, Sci. Results*. College Station, TX (Ocean Drilling Program), 159, 199-207.

Agnini, C., Fornaciari, E., Raffi, I., Catanzariti, R., Pälike, H., Backman, J., & Rio, D. (2014). Biozonation and biochronology of Paleogene calcareous nannofossils from low and middle latitudes. *Newsletters on Stratigraphy*, 47, 131-181.

Agterberg, F. P., 1990. *Automated Stratigraphic Correlation*. Elsevier, Amsterdam, 424 pp.

Agterberg, F. P., and Gradstein, F. M., 1997a, Measuring the relative importance of fossil events in quantitative stratigraphy. In: Pawlowski-Glahn, V., (Ed), *Proceedings IAMH 1997*, CIMNB Barcelona, Part 1, 349-354.

Agterberg, F. P., and Gradstein, F. M., 1997b. Sequencing, scaling, and correlation of stratigraphic events. In: Naiwen, W., Remane, J., (Eds), *Proceedings 30th International Geologic Congress*, 11, Beijing, China, VCP, Zeist, 29-37.

Agterberg, F. P., and Gradstein, F. M., 1999. The RASC method for ranking and scaling of biostratigraphic events. *Earth Science Reviews*, 46, 1–25.

Agterberg, F. P., Gradstein, F. M., Cheng, Q., 1999. Stratigraphic correlation on the basis of fossil events. In: Buccianti, A. et al., (Eds), *Proceedings 4th Annual Conference International Association of Mathematics Geological Ischia*, October 1998, 743-748.

Berggren, W. A., Kent, D. V., Swisher, C. C., III and Aubry, M.-P., 1995. A revised Cenozoic Geochronology and Chronostratigraphy. In: Berggren, W. A., Kent, D. V., Aubry, M.-P. and Hardenbol, J., Eds., *Geochronology, Time scales and Global Stratigraphic Correlations: A Unified Temporal Framework for an Historical Geology*, Society of Economic Geologists and Mineralogists Special Paper 54, 129-212.

Bowman, A. R. (2011). Building a high resolution calcareous nannofossil biozonation using ranking and scaling (RASC). University of Nebraska-Lincoln, Ph.D. dissertation, https://digitalcommons.unl.edu

Bown, P.R. (2005). Cenozoic calcareous nannofossil biostratigraphy, ODP Leg 198 Site 1208 (Shatsky Rise, northwest Pacific Ocean), P*roc. ODP, Sci. Results*. College Station, TX (Ocean Drilling Program), 198, 1–44.

Bukry, D., 1972. Coccolith stratigraphy—Leg 14, Deep Sea Drilling Project, *Init. Repts. DSDP*, 14: Washington (U.S. Govt. Printing Office), 487-494.

Bukry, D. (1973). Low-latitude coccolith biostratigraphic zonation, *Init. Repts. DSDP*, 14: Washington (U.S. Govt. Printing Office),, 15, 685-703.

De Kaenel, E., & Villa, G. (1996). Oligocene-Miocene calcareous nannofossil biostratigraphy and paleoecology from the Iberia Abyssal Plain. In *Proc. Ocean Drilling Program Scientific Results*, 79-146 pp.

Fornaciari, E., Raffi, I., Rio, D., Villa, G., Backman, J., & Olafsson, G. (1990). Quantitative distribution patterns of Oligocene and Miocene calcareous nannofossils from the western equatorial Indian Ocean*, Proc. ODP, Sci. Results*. College Station, TX (Ocean Drilling Program), 115, 237-254.

Fornaciari, E., Backman, J., & Rio, D. (1993). Quantitative distribution patterns of selected lower to middle Miocene calcareous nannofossils from the Ontong Java Plateau, *Proc. ODP, Sci. Results*. College Station, TX (Ocean Drilling Program),, 130, 245-256.

Fornaciari, E. & Rio, D. (1996). Latest Oligocene to early middle Miocene quantitative calcareous nannofossil biostratigraphy in the Mediterranean region. *Micropaleontology*, 1, 1-36.

Gartner, S., 1992. Miocene nannofossil chronology in the North Atlantic DSDP Site 608. *Marine Micropaleontology* 18, 307–331.

Gradstein, F. M., and Agterberg, F. P., 1982. Models of Cenozoic foraminiferal stratigraphy-northwestern Atlantic margin. In: Cubitt, J. M., Reyment, R. A., (Eds), Quantitative Stratigraphic Correlation, Wiley, Chichester, 119-173.

Gradstein, F. M., Agterberg, F. P., and D'iorio, M. A., 1990. Time in quantitative stratigraphy. In: Cross, T. A., (Ed), *Quantitative Dynamic Stratigraphy*, Englewood Cliffs, New Jersey, Prentice Hall, 519–542.

Gradstein, F. M., and Agterberg, F. P., 1998. Uncertainty in stratigraphic correlation. In: Gradstein, F. M. et al., (Eds), *Sequence Stratigraphy-Concepts and Applications*, Elsevier, Amsterdam, 9-29.

Gradstein, F.M., Ogg, J.G., Schmitz, M.D., and Ogg, G.M., Eds., 2012. *The Geological Time Scale 2012*. Amsterdam: Elsevier, 1144p.

Hammer, Ø., Harper, D. A. T., & Ryan, P. D. (2001). PAST: Paleontological Statistics Software Package for education and data analysis. *Palaeontologica Electronica* 4.

Haq, B. U., Hardenbol, J., & Vail, P. R. (1987). Chronology of fluctuating sea levels since the Triassic. *Science*, *235*(4793), 1156-1167.

Maiorano, P., & Monechi, S. (1998). Revised correlations of Early and Middle Miocene calcareous nannofossil events and magnetostratigraphy from DSDP Site 563 (North Atlantic Ocean). *Marine micropaleontology*, *35*(3), 235-255.

Marino, M., & Flores, J. A. (2002). Miocene to Pliocene calcareous nannofossil biostratigraphy at ODP Leg 177 Sites 1088 and 1090. *Marine Micropaleontology*, *45*(3), 291-307.

Martini, E. (1971). Standard Tertiary and Quaternary calcareous nannoplankton zonation. In Farinacci, A. (Ed.), *Proc. 2nd Int. Conf. Planktonic Microfossils Roma*: Rome (Ed. Tecnosci.), 2:739–785.

Mârunteanu, M. (1999). Litho-and Biostratigraphy (Calcareous Nannoplankton) Of The Miocene Deposits. from The Outer Moldavides. *Geologica Carpathica*, *50*(4).

Okada, H., & Bukry, D. (1980). Supplementary modification and introduction of code numbers to the low-latitude coccolith biostratigraphic zonation (Bukry, 1973; 1975). *Marine Micropaleontology*, *5*, 321-325.

Olafsson, G. (1989). Quantitative calcareous nannofossil biostratigraphy of upper Oligocene to middle Miocene sediment from ODP Hole 667A and middle Miocene sediment from DSDP Site 574, *Proc. ODP, Sci. Results*. College Station, TX (Ocean Drilling Program), 108, 9-22.

Parker, M. E., Clark, M., & Wise, S. W. Jr. (1985). Calcareous Nannofossils of Deep Sea Drilling Project Site-558 and Site-563, North Atlantic Ocean Biostratigraphy and The Distribution of Oligocene Braarudosphaerids. *Init. Repts. DSDP*, 14: Washington (U.S. Govt. Printing Office), *82*, 559-589.

Pujos, A., 1985. Cenozoic nannofossils, central equatorial Pacific, Deep Sea Drilling Project Leg 85, *Init. Repts. DSDP*, 14: Washington (U.S. Govt. Printing Office), 581-608.

Raffi, I., and Flores, J.-A., 1995. Pleistocene through Miocene calcareous nannofossils from eastern equatorial Pacific Ocean (Leg 138), *Proc. ODP, Sci. Results*. College Station, TX (Ocean Drilling Program), 233–286.

Raffi, I., Backman, J., Fornaciari, E., Pälike, H., Rio, D., Lourens, L., & Hilgen, F. (2006). A review of calcareous nannofossil astrobiochronology encompassing the past 25 million years. *Quaternary Science Reviews*,*25*(23), 3113-3137.

Rio, D., Fornaciari, E., Raffi, I. (1990). Late Oligocene through early Pleistocene calcareous nannofossils from western equatorial Indian Ocean (Leg 115). In *Proc. ODP, Sci. Results*. College Station, TX (Ocean Drilling Program),, 115, 175-235.

Shafik, S., Watkins, D. K., & Shin, I. C. (1998). Upper Cenozoic Calcareous Nannofossil Biostratigraphy Côte d'Ivoire-Ghana Margin, Eastern Equatorial Atlantic. *Proc. ODP, Sci. Results*, College Station, TX (Ocean Drilling Program), 159, 413–431

Shipboard Scientific Party (2004). Site 1264. In Zachos, J.C., Kroon, D., Blum, P., et al., *Proc. ODP, Init. Repts.*, 208: College Station, TX (Ocean Drilling Program), 1–73.

Shipboard Scientific Party (2004). Site 1265. In Zachos, J.C., Kroon, D., Blum, P., et al., *Proc. ODP, Init. Repts.*, 208: College Station, TX (Ocean Drilling Program), 73–107

Steininger, F. F., Aubry, M. P., Berggren, W. A., Biolzi, M., Borsetti, A. M., Cartlidge, J. E., Cati, R., Corfield, R., Gelati, R., 1acarino, S., Napoleone, C., Ottner, E., Rögl, F., Roetzel, R., Spezzaferri, S., Tateo, F., Villa, G., & Zevenboom, D. (1997). The global stratotype section and point (GSSP) for the base of the Neogene. *Episodes*, *20*, 23-28.

Styzen, M.J., 1997. Cascading counts of nannofossil abundance. *J. Nannoplankton Res.* 19 (1), 49.

Takayama, T , and Sato, T., 1985. Coccolith biostratigraphy of the North Atlantic Ocean, Deep Sea Drilling Project Leg 94. *In* Ruddiman, W. R, Kidd, R. B., Thomas, E., et al., *Init. Repts. DSDP*, 14: Washington (U.S. Govt. Printing Office), 94, 651-702.

Turco, E., Cascella, A., Gennari, R., Hilgen, F. J., Iaccarino, S. M., & Sagnotti, L. (2011). Integrated stratigraphy of the La Vedova section (Conero Riviera, Italy) and implications for the Burdigalian/Langhian boundary.*Stratigraphy*, *8*(2), 89.

Watkins, D. K., Shafik, S., & Shin, I. C. (1998). Calcareous nannofossils from the Cretaceous of the Deep Ivorian Basin. . *Proc. ODP, Sci. Results*, College Station, TX (Ocean Drilling Program), 159, 319–333

Watkins, D. K., & Bergen, J. A. (2003). Late Albian adaptive radiation in the calcareous nannofossil genus Eiffellithus. *Micropaleontology*, *49*(3), 231-251.

Young, J. R., Bergen, J. A., Bown, P. R., Burnett, J. A., Fiorentino, A., Jordan, R. W., & Von Salts, K. (1997). Guidelines for coccolith and calcareous nannofossil terminology. *Palaeontology*, *40*(4), 875-912.

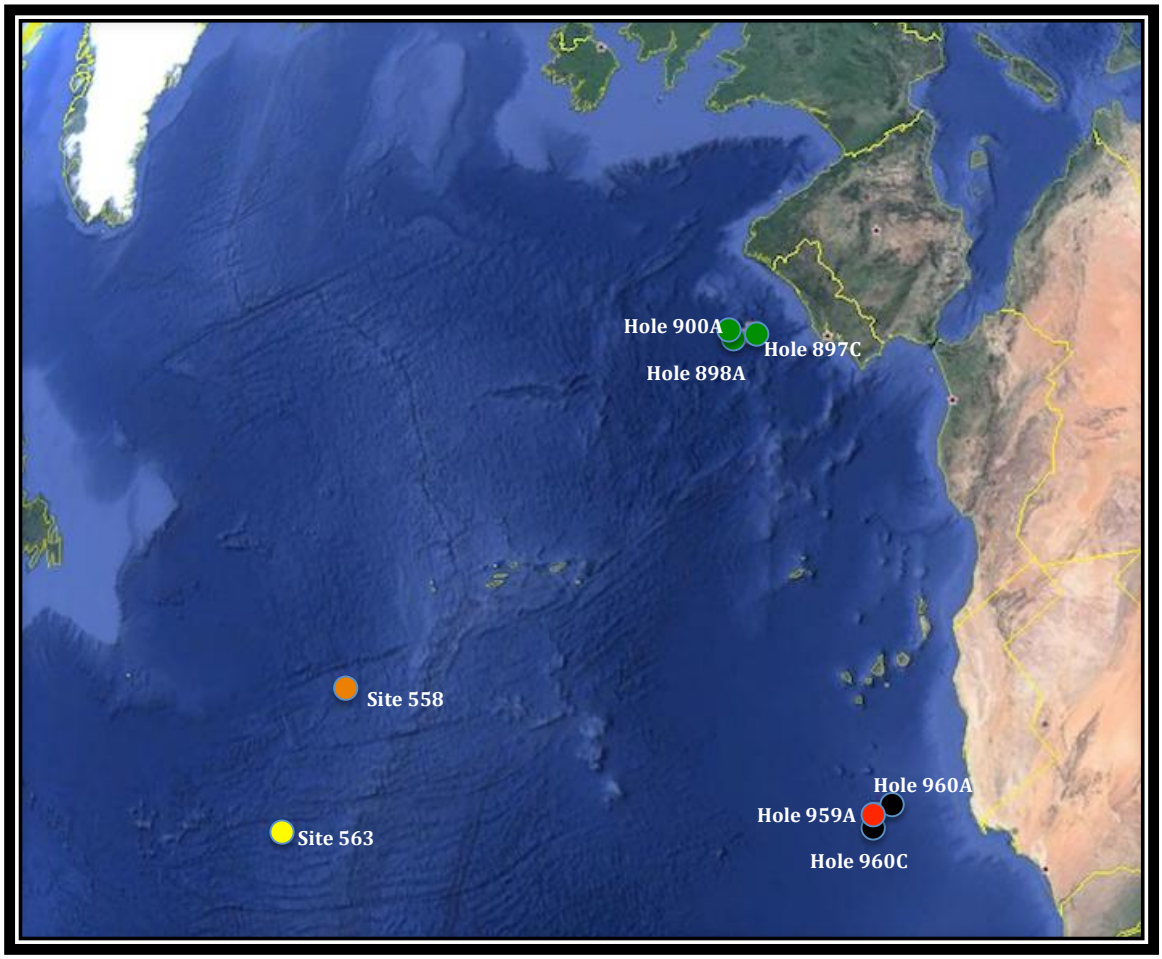

Fig.1: Location map (Source: Google earth version 7.1.2.2041).

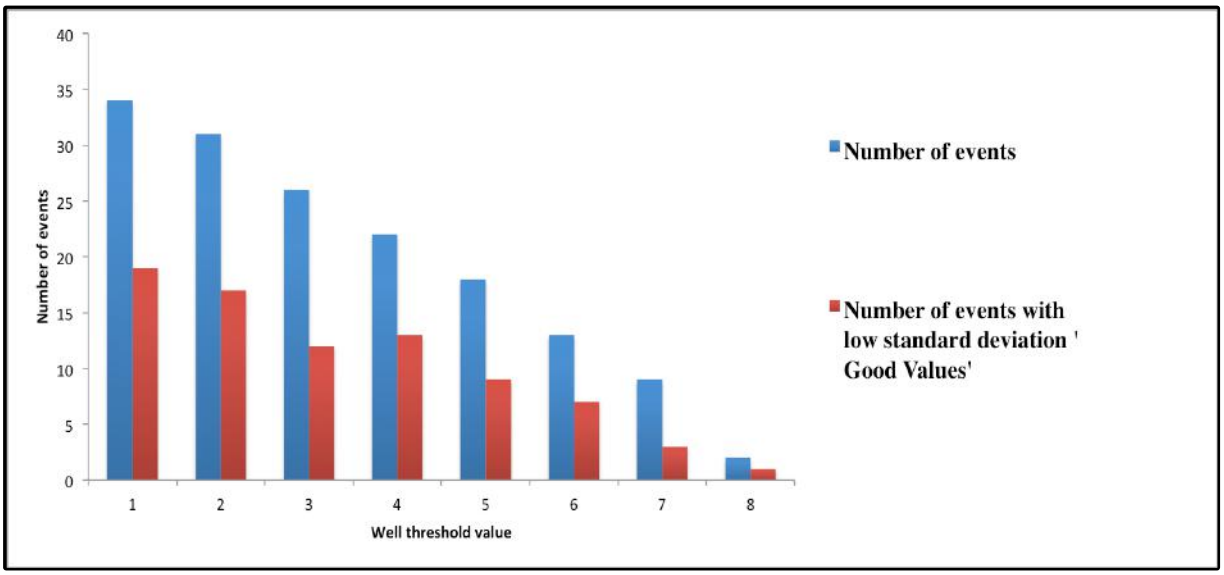

Fig.2: Number of events resulted from the different RASC runs.

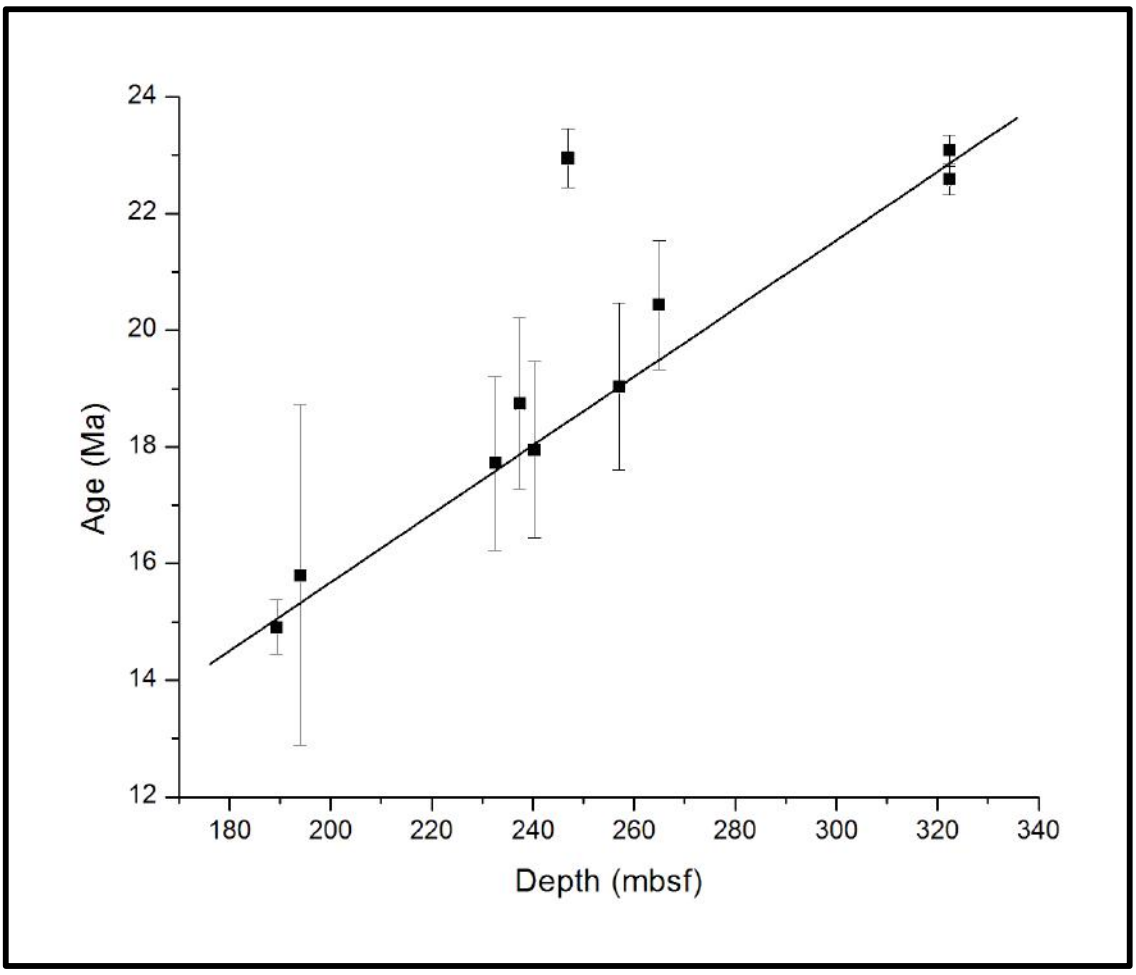

Figure 3: Age/Depth model for Hole 959A. Values used for this plot from Table 3a. Note: Age Error bars represent lower/upper limits for age reported from Raffi et al., (2006) and GTS 2012.

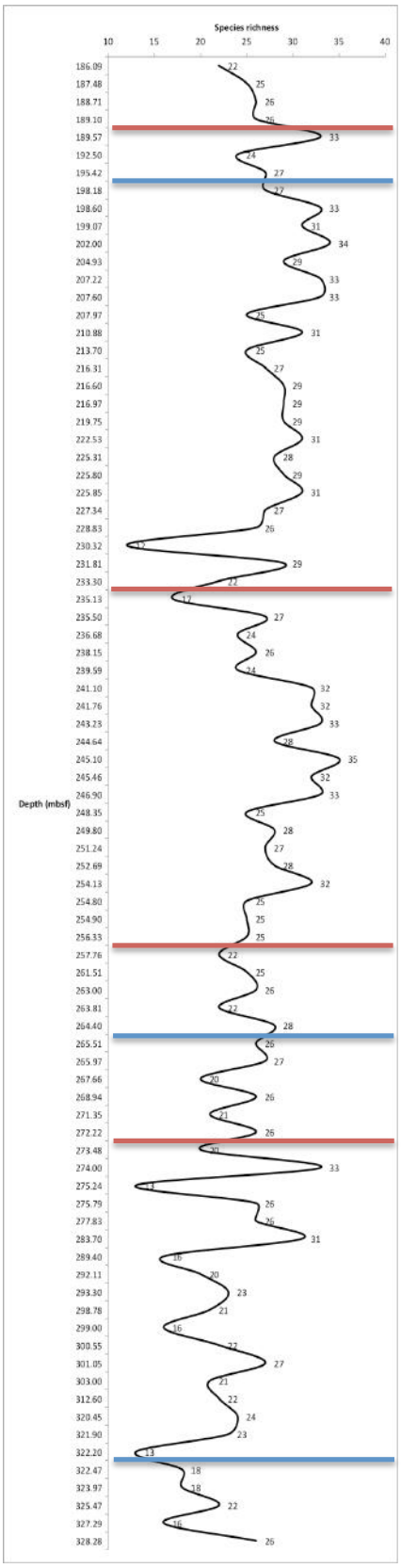

Datum	Marker events
Base of CN4 Zone	Based on the LO of *H. ampliaperta*
Base of Langhian	Approximated by the LCO of *D. deflandrei*
Base of CN3	Based on the FCO of *S. heteromorphus*
Base of CN2 Zone	Based on the FO of *S. belemnos*
Base of Burdigalian	Provisionally placed based on the FO of *H. ampliaperta*
Base of CN1c	Based on the FO of *O. serratus*
Oligocene - Miocene boundary (Base of Aquitanian stage)	Approximated by the LO of *S. delphix*

Fig.4: Species richness (count of different species per sample) in Hole 959A.

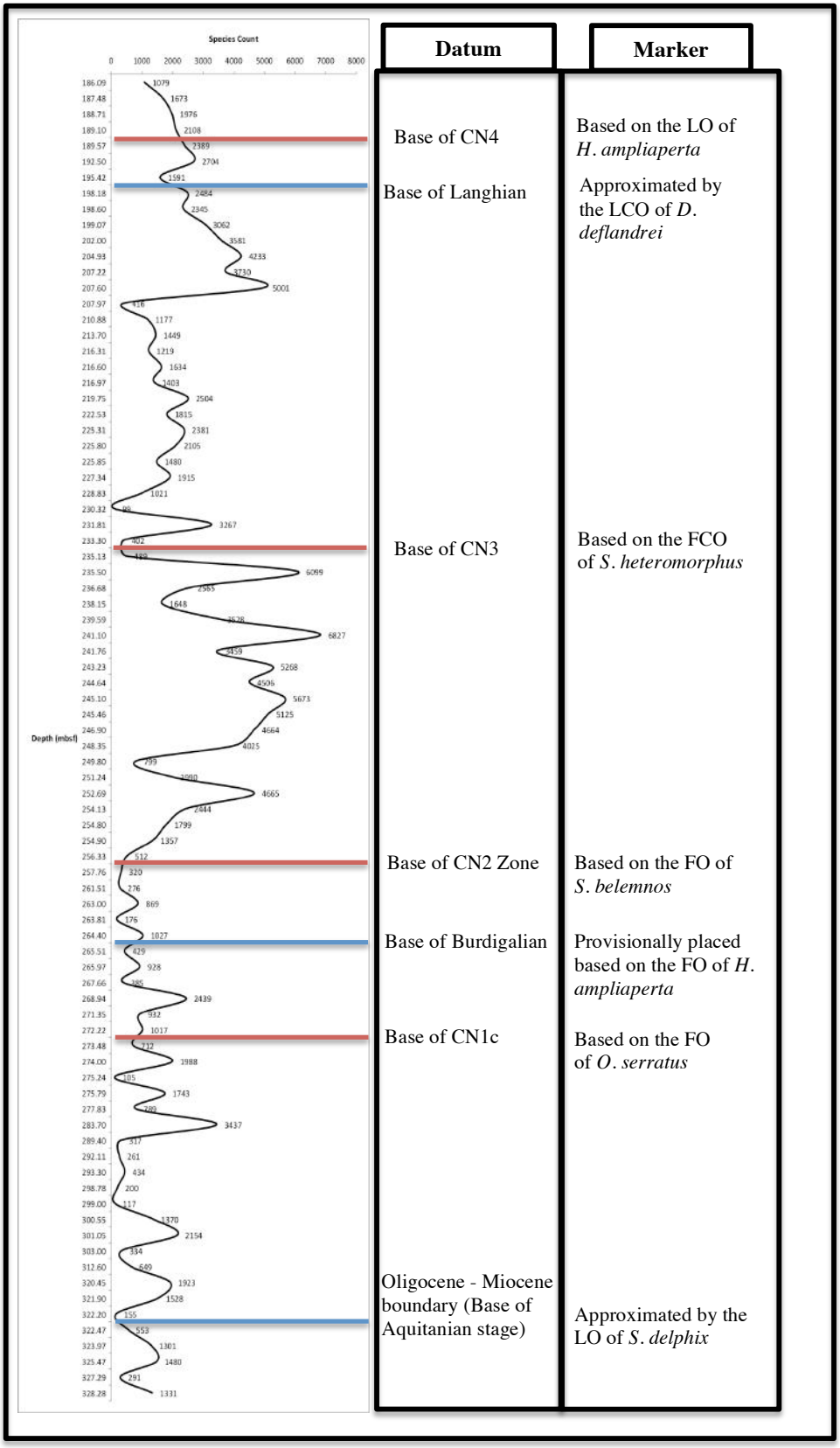

Fig.5: Species counts per sample in Hole 959A.

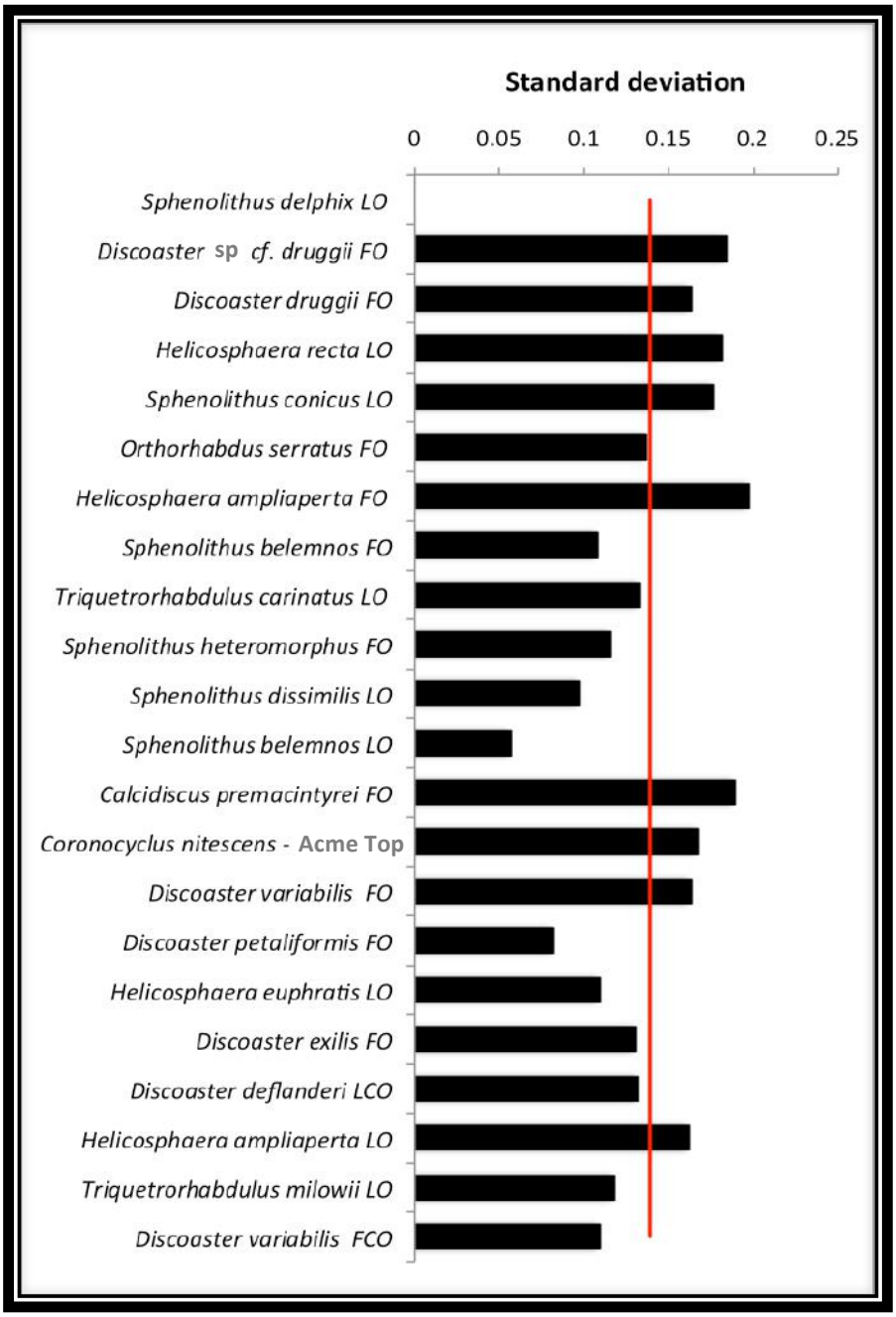

Fig.6: RASC results with the standard deviation of scaled events, with a well threshold 'k'=4, compared to the average standard deviation of 0.1389.

Bioevent/Biohorizon	Dephs (mbsf)		
	Depth interval		Average
FO *Calcidiscus premacintyrei*	245.10	245.46	245.28
F-Acme *Coronocyclus nitescens*	254.90	256.33	255.62
L-Acme *Coronocyclus nitescens*	235.15	235.50	235.33
L-Acme *Cyclicargolithus floridanus*	192.50	195.42	193.96
LO *Discoaster adamanteus*	241.10	241.76	241.43
LO *Discoaster deflandrei*	187.48	188.71	188.10
LCO *Discoaster deflandrei*	192.50	195.42	193.96
FO *Discoaster druggii*	244.64	245.10	244.87
FO *Discoaster* sp. *cf D. druggii*	268.94	271.35	270.15
FCO *Discoaster* sp. *cf D. druggii*	245.46	246.90	246.18
FO *Discoaster exilis*	233.30	235.13	234.22
FCO *Discoaster exilis*	227.34	228.83	228.09
FO *Discoaster musicus*	187.48	188.71	188.10
FO *Discoaster variabilis*	235.13	235.50	235.32
FCO *Discoaster variabilis*	227.34	228.83	228.09
FCO *Discoaster petaliformis*	207.60	207.97	207.79
FO *Helicosphaera ampliaperta*	264.40	265.51	264.96
LO *Helicosphaera ampliaperta*	189.10	189.57	189.34
LO *Helicosphaera euphratis*	189.10	189.57	189.34
FCO *Helicosphaera mediterranea*	216.97	219.75	218.36
FO *Orthorhabdus serratus*	274.00	275.24	274.62
FCO *Orthorhabdus serratus*	272.22	273.48	272.85
FO *Sphenolithus belemnos*	256.33	257.76	257.05
LO *Sphenolithus belemnos*	239.59	241.10	240.35
FO *Sphenolithus heteromorphus*	245.10	245.46	245.28
FCO *Sphenolithus heteromorphus*	233.30	235.13	234.22
LO *Sphenolithus dissimilis*	261.51	263.00	262.26
FO *Sphenolithus disbelmnos*	322.20	322.47	322.34
LO *Sphenolithus disbelemnos*	225.80	225.85	225.83
LO *Sphenolithus delphix*	322.20	322.47	322.34
LO *Triquetrorhabdulus carinatus*	236.68	238.15	237.42
LO *Triquetrorhabdulus milowii*	189.57	192.50	191.04
F-Acme Umbilicophaera sp.#2	254.90	256.33	255.62

Table.1: Summary of events in Hole 959A. FO= First Occurrence datum, LO= Last Occurrence datum, FCO= First Common datum, LCO= Last Common datum, F-Acme= Beginning of an Acme, and L-Acme= End of an Acme.

Well threshold value	Total number of events	Number of good events (Lower S.d)	Percentage of Good values compared to the overall number of events
1	34	19	55.88
2	31	17	54.84
3	26	12	46.15
4	22	13	59.09
5	18	9	50.00
6	13	7	53.85
7	9	3	33.33
8	2	1	50.00

Table.2: Results from different RASC runs with different well threshold values. Well threshold value=4 is selected subjectively because of the high percentage of low standard deviation event compared to the overall number of event.

Bioevent	Ave. Age (Ma)	Ave.Depth (mbsf)
LO *Sphenolithus delphix*	23.08	322.34
FO *Discoaster druggii*	22.82	244.87
FO *Sphenolithus disbelmnos*	22.59	322.34
FO *Helicosphaera ampliaperta*	20.43	264.96
FO *Sphenolithus belemnos*	19.03	257.05
LO *Triquetrorhabdulus carinatus*	18.28	237.42
LO *Sphenolithus belemnos*	17.95	240.35
FCO *Sphenolithus hetermorphous*	17.71	234.22
LCO *Discoaster deflandrei*	15.80	193.96
LO *Helicosphaera ampliaperta*	14.91	189.34

Table 3a: List of bioevents used to plot Age/Depth model (Figure 3) for Hole 959A. Age values are taken from GTS2012 and Raffi et al., (2006). Note: Ave. depth values are the average values of the interval in which the event exist in Hole 959A (taken from Table 1).

Bioevent	Interpolated Age values (Ma)	Ave. Depth (mbsf)
FO *Calcidiscus premacintyrei*	18.30	245.28
F-Acme *Coronocyclus nitescens*	18.90	255.62
L-Acme *Coronocyclus nitescens*	17.72	235.33
L-Acme *Cyclicargolithus floridanus*	15.30	193.96
LO *Discoaster adamanteus*	18.07	241.43
LO *Discoaster deflandrei*	14.95	188.10
FO *Discoaster* sp. *cf D. druggii*	19.75	270.15
FCO *Discoaster* sp. *cf D. druggii*	18.35	246.18
FO *Discoaster exilis*	17.65	234.22
FCO *Discoaster exilis*	17.29	228.09
FO *Discoaster musicus*	14.95	188.10
FO *Discoaster variabilis*	18.30	245.28
FCO *Discoaster variabilis*	17.29	228.09
FCO *Discoaster petaliformis*	16.11	207.79
LO *Helicosphaera euphratis*	15.03	189.34
FCO *Helicosphaera mediterranea*	16.72	218.36
FO *Orthorhabdus serratus*	20.01	274.62
FCO *Orthorhabdus serratus*	19.91	272.85
LO *Sphenolithus dissimilis*	19.29	262.26
LO *Sphenolithus disbelemnos*	17.16	225.83
LO *Triquetrorhabdulus milowii*	15.13	191.04

Table 3b: Interpolated age values for secondary events in Hole 959A. Age values were interpolated using the linear relationship from the Age/Depth model (Figure 3). Linear equation (Y = 0.0585X +3.9496) X= Depth, Y= Age.

Event/Site	Hole 959A	Hole 563	Hole 558	Hole 897C	Hole 898A	Hole 900A	Hole 960A	Hole 960C	Average
FO *Calcidiscus premacintyrei*	18.298	15.864	19.025	22.465	18.016				18.734
F-Acme *Coronocyclus nitescens*	18.903	19.329					22.450		20.227
L-Acme *Coronocyclus nitescens*	17.716	17.493	17.147		17.387		20.852		18.119
L-Acme *Cyclicargolithus floridanus*	15.296	14.221	7.808	22.209	17.321	9.406	15.720		14.569
LO *Discoaster adamanteus*	18.073			22.845			19.234		20.051
LO *Discoaster deflandrei*	14.953						12.617	14.532	14.034
FO *Discoaster* sp. *cf D. druggii*	19.753			23.025	22.381		22.748		21.977
FCO *Discoaster* sp. *cf D. druggii*	18.351								18.351
FO *Discoaster exilis*	17.651		16.173		17.583	17.082	15.134	18.384	17.001
FCO *Discoaster exilis*	17.293							15.638	16.465
FO *Discoaster musicus*	14.953				17.285				16.119
FO *Discoaster variabilis*	18.298		16.457		18.214		17.919	15.638	17.305
FCO *Discoaster variabilis*	17.293				17.293		12.740	12.971	15.074
FCO *Discoaster petaliformis*	16.105			20.788			15.720	17.590	17.551
LO *Helicosphaera euphratis*	15.026			22.756	20.091	20.613	15.720	15.638	18.307
FCO *Helicosphaera mediterranea*	16.724			22.960					19.842
FO *Orthorhabdus serratus*	20.015	22.491		22.676	19.556	19.817	20.852	21.590	20.999
FCO *Orthorhabdus serratus*	19.911								19.911
LO *Sphenolithus dissimilis*	19.292	18.900		22.615	18.358	17.448	16.787	18.829	18.890
LO *Sphenolithus disbelemnos*	17.160	19.718							18.439
LO *Triquetrorhabdulus milowii*	15.125	9.871	15.309		17.386	15.199	12.617	13.207	14.102

Table.4: Interpolated age values for secondary events from the linear relationship of the Age/Depth model for all Sites/Holes in this study. (Equations used in the interpolation of age values are listed in Appendix 3)

Event	S.d (Ave = 0.1389)	Number of Wells (out of 8)
Sphenolithus delphix LO	0	4
Discoaster sp *cf. D. druggii* FO	0.1843	4
Discoaster druggii FO	0.1633	7
Helicosphaera recta LO	0.1815	6
Sphenolithus conicus LO	0.1764	5
Orthorhabdus serratus FO	0.137	7
Helicosphaera ampliaperta FO	0.1976	7
Sphenolithus belemnos FO	0.1081	7
Triquetrorhabdulus carinatus LO	0.1332	8
Sphenolithus heteromorphus FO	0.1159	8
Sphenolithus dissimilis LO	0.09762	7
Sphenolithus belemnos LO	0.05683	7
Calcidiscus premacintyrei FO	0.1893	5
Coronocyclus nitescens - Acme Top	0.1678	5
Discoaster variabilis FO	0.1632	5
Discoaster petaliformis FO	0.08227	4
Helicosphaera euphratis LO	1.10E-01	6
Discoaster exilis FO	0.1306	6
Discoaster deflandrei LCO	0.1322	5
Helicosphaera ampliaperta LO	0.1622	6
Triquetrorhabdulus milowii LO	0.1181	7
Discoaster variabilis FCO	0.1096	4

Table.5: The final optimum sequence results from RASC run with well threshold value = 4. Highlighted rows represent good values (i.e., events with low standard deviation)

Plate 1

1. *Calcidiscus* spp., crossed polarized light, sample 30X-2, 30-31

2. *Coccolithus pelagicus,* crossed polarized light, sample 32X-5, 125-126

3. *Coronocyclus nitenses,* crossed polarized light, sample 32X-5, 125-126

4. *Cyclicarglithus floridanus*, crossed polarized light, sample 32X-5, 125-126

5. *Dictyococcytes* spp. (medium), crossed polarized light, sample 32X-6, 25-26

6. *Discoaster aulakos,* phase contrast, sample 27X-1, 37-38

7. *Discoaster deflandrei,* plane light, sample 32X-5, 125-126

8. *Discoaster druggii,* Plane light, sample 26X-6, 37-38

9. *Discoaster exilis,* plane light, sample 21X-7, 30-31

10a. *Discoaster petaliformis,* Plane light, sample 20XCC

10b. *Discoaster petaliformis,* Plane light, sample 20XCC, same specimen as above with different focus.

11. *Discoaster* sp. *cf D. druggii,* phase contrast, sample 27X-1, 37-38

Plate 1

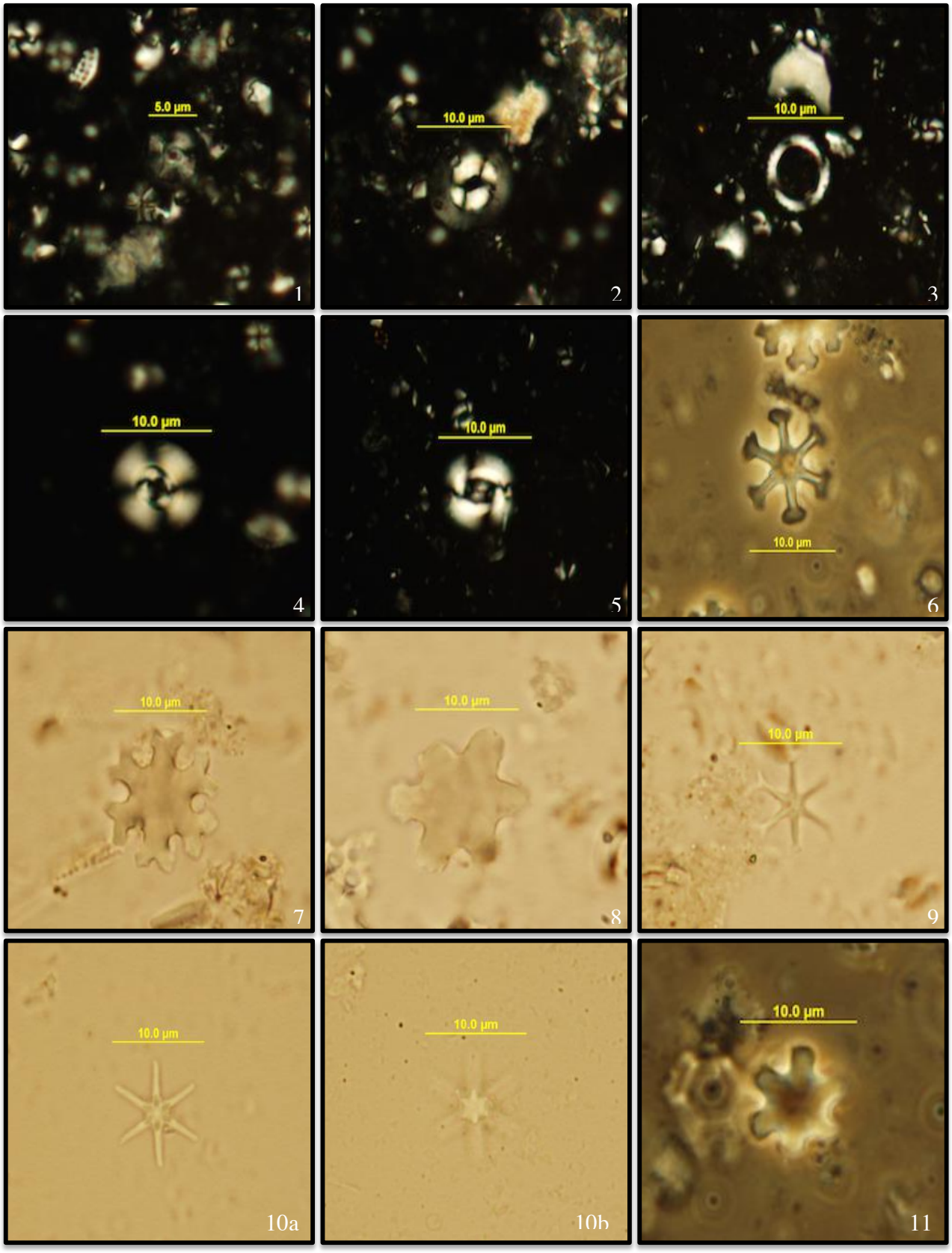
5.0 µm
1
10.0 µm
2
10.0 µm
3
10.0 µm
4
10.0 µm
5
10.0 µm
6
10.0 µm
7
10.0 µm
8
10.0 µm
9
10.0 µm
10a
10.0 µm
10b
10.0 µm
11

Plate 2

1. *Discoaster variabilis,* plane light, sample 21X-7, 30-31

2. *Hayster perplexus,* phase contrast, sample 22X-1, 48-49

3. *Helicosphaera ampliaperta,* crossed polarized light, sample 22X-5, 48-49

4. *Helicosphaera carteri,* crossed polarized light, sample 27X-6, 37-38

5. *Helicosphaera euphratis,* crossed polarized light, sample 34X-6, 44-45

6. *Helicosphaera intermedia,* crossed polarized light, sample 22X-7, 33-34

7. *Helicosphaera mediterranea,* crossed polarized light, sample 27X-6, 37-38

8a. *Helicosphaera obliqua,* crossed polarized light, sample 21X-7, 30-31

8b. *Helicosphaera obliqua,* plane light, sample 21X-7, 30-31

9. *Helicosphaera* sp. cf *H. lophota,* crossed polarized light, sample 33XCC

10. *Helicosphaera* sp. cf *H. recta,* crossed polarized light, sample 35X-5, 8-10

11. *Orthorhabdus serratus,* crossed polarized light, sample 29X-3, 38-40

Plate 2

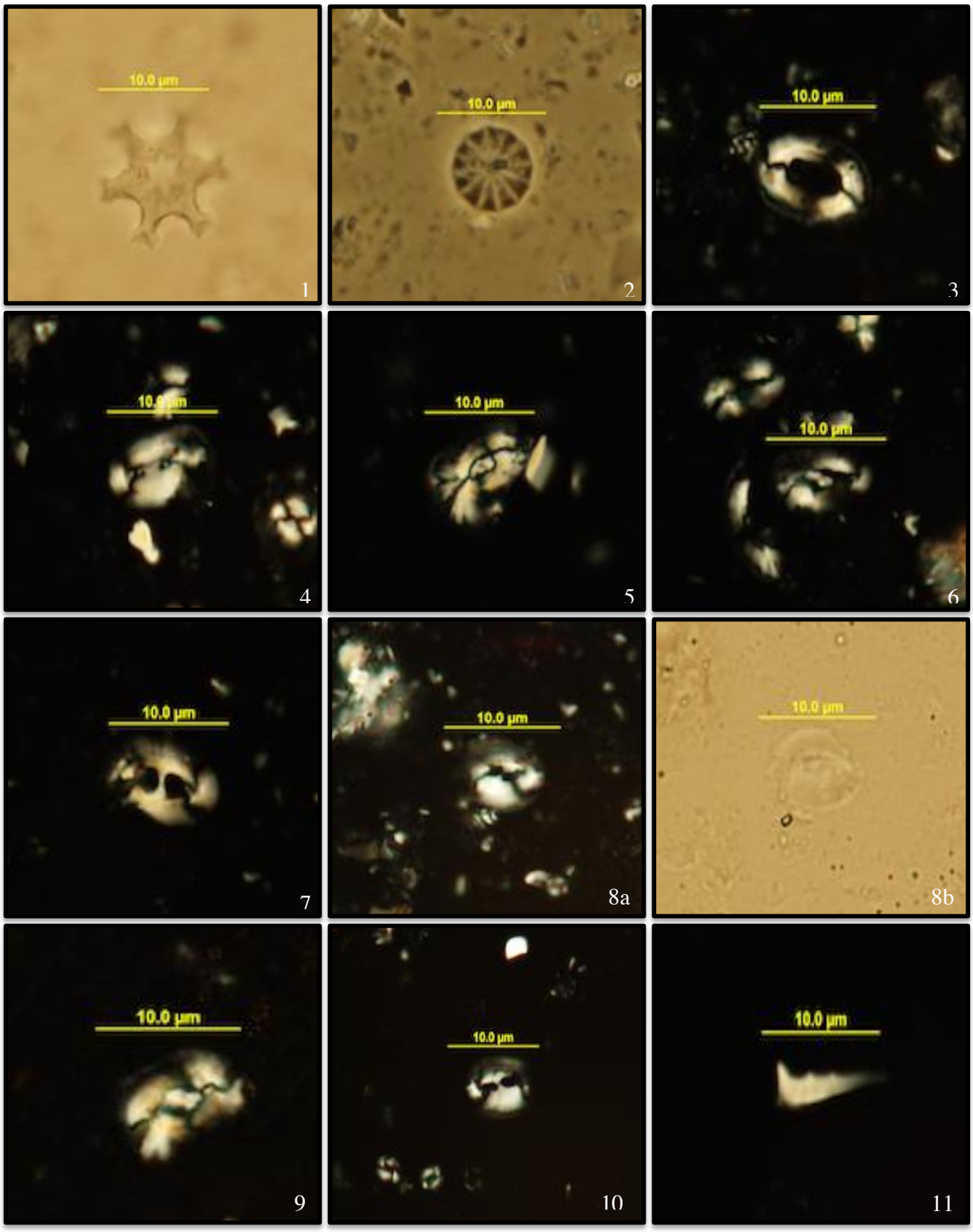
10.0 µm
1
10.0 µm
2
10.0 µm
3
10.0 µm
4
10.0 µm
5
10.0 µm
6
10.0 µm
7
10.0 µm
8a
10.0 µm
8b
10.0 µm
9
10.0 µm
10
10.0 µm
11

Plate 3

1. *Pontosphaera multipora,* crossed polarized light, sample 22X-7, 33-34

2. *Reticulofenstra* spp. (medium), crossed polarized light, sample 30XCC

3. *Reticulofenstra* spp. (small), crossed polarized light, sample 30XCC

4. *Reticulofenstra* spp. (v. small), crossed polarized light, sample 30XCC

5. *Scyphosphaera* spp., crossed polarized light, sample 24X-5, 40-41

6. *Solidopons petrae,* crossed polarized light, sample 22X-5, 48-49

7a. *Sphenolithus belemnos,* crossed polarized light, 0º, sample 27X-6, 37-38

7b. *Sphenolithus belemnos,* crossed polarized light, 45º, sample 27X-6, 37-38

8a. *Sphenolithus conicus,* crossed polarized light, 0º, sample 30XCC

8b. *Sphenolithus conicus,* crossed polarized light, 45º, sample 30XCC

9a. *Sphenolithus delphix,* crossed polarized light, 0º, sample 35X5, 8-10

9b. *Sphenolithus delphix,* crossed polarized light, 45º, sample 35X5, 8-10

Plate 3

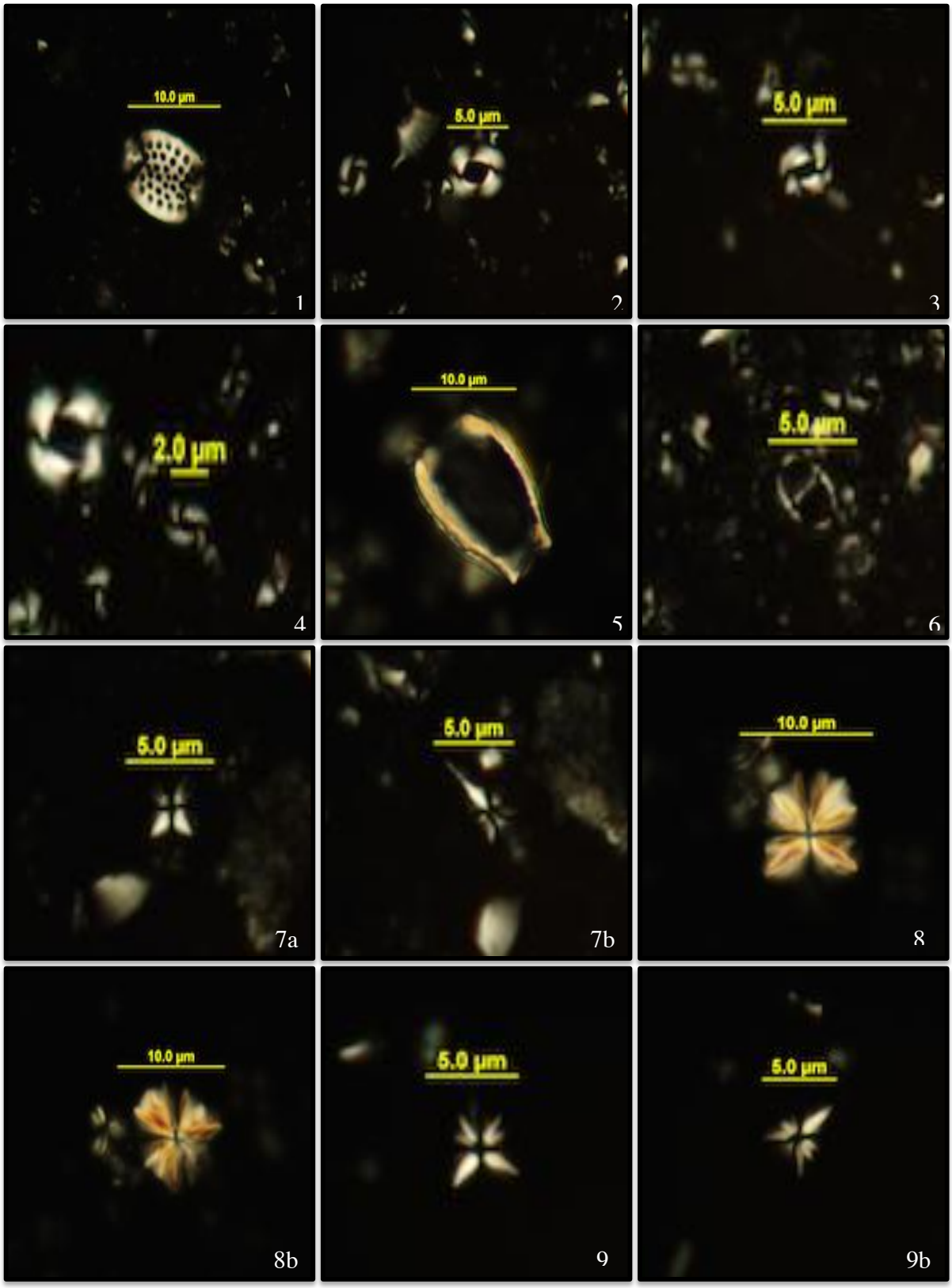
10.0 µm
1
5.0 µm
2
5.0 µm
3
2.0 µm
4
10.0 µm
5
5.0 µm
6
5.0 µm
7a
5.0 µm
7b
10.0 µm
8
10.0 µm
8b
5.0 µm
9
5.0 µm
9b

Plate 4

1a. *Sphenolithus delphix,* crossed polarized light, 0º, sample 33XCC

1b. *Sphenolithus delphix,* crossed polarized light, 45º, sample 33XCC

2a. *Sphenolithus disbelemnos,* crossed polarized light, 0º, sample 34X-6, 44-45

2b. *Sphenolithus disbelemnos,* crossed polarized light, 45º, sample 34X-6, 44-45

3a. *Sphenolithus dismilis,* crossed polarized light, 0º, sample 33XCC

3b. *Sphenolithus dismilis,* crossed polarized light, 45º, sample 33XCC

4a. *Sphenolithus heteromorphus,* crossed polarized light, 0º, sample 22X-7, 33-34

4b. *Sphenolithus heteromorphus,* crossed polarized light, 45º, sample 22X-7, 33-34

5a. *Sphenolithus moriformis* crossed polarized light, 0º, sample 30XCC

5b. *Sphenolithus moriformis,* crossed polarized light, 45º, sample 30XCC

6a. *Sphenolithus umberellus,* crossed polarized light, 0º, sample 30XCC

6b. *Sphenolithus umberellus,* crossed polarized light, 45º, sample 30XCC

Plate 4

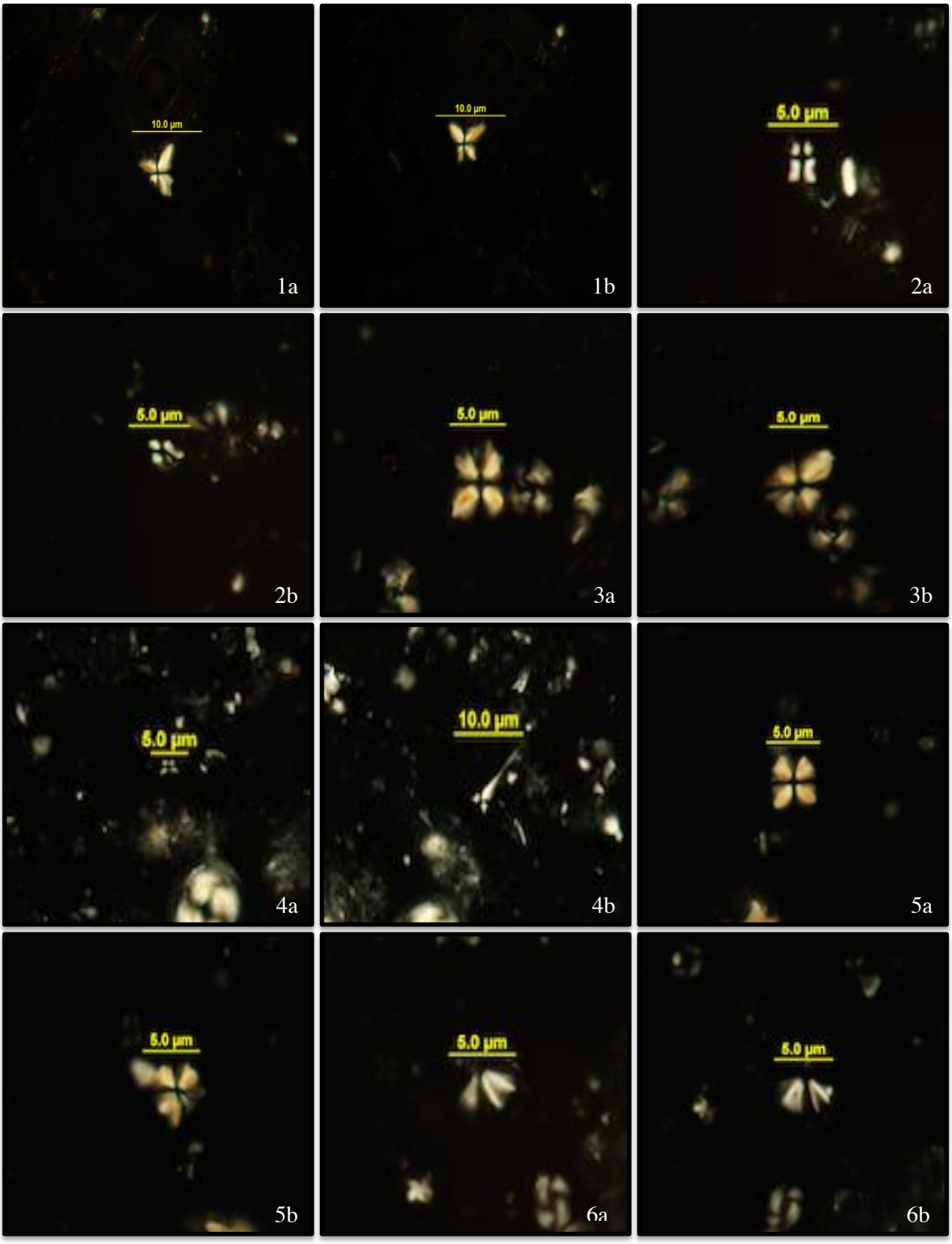
10.0 µm
1a
10.0 µm
1b
5.0 µm
2a
5.0 µm
2b
5.0 µm
3a
5.0 µm
3b
5.0 µm
4a
10.0 µm
4b
5.0 µm
5a
5.0 µm
5b
5.0 µm
6a
5.0 µm
6b

Plate 5

1. *Tetralithoides symeonidesii,* crossed polarized light, sample 21XCC

2. *Triquetrorhabdulus carinatus,* crossed polarized light, sample 32X-5, 125-126

3. *Triquetrorhabdulus carinatus,* crossed polarized light, sample 35X-4, 59-60

4. *Triquetrorhabdulus longus,* crossed polarized light, sample 29XCC

5. *Triquetrorhabdulus milowii,* crossed polarized light, sample 26X-4, 120-121

6. *Umbilicosphaera cf* sp. #1, crossed polarized light, sample 22X-7, 33-34

7. *Umbilicosphaera cf* sp. #2, crossed polarized light, sample 22X-7, 33-34

8. Unidenified sp. Type#1, crossed polarized light, sample 21XCC

9. Unidenified sp. Type#2, crossed polarized light, sample 32X-6, 25-26

Plate 5

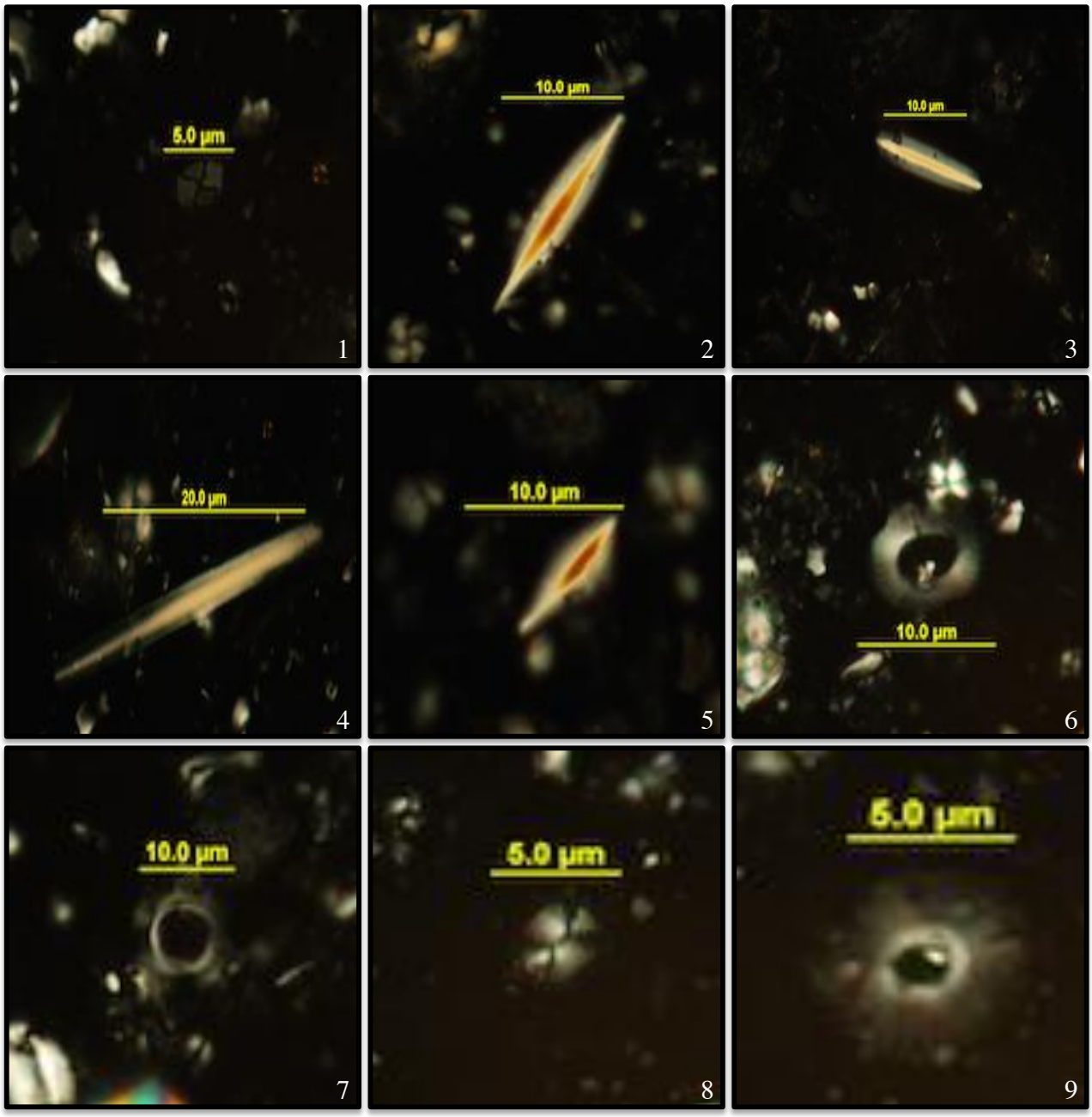
5.0 µm
1
10.0 µm
2
10.0 µm
3
20.0 µm
4
10.0 µm
5
10.0 µm
6
10.0 µm
7
5.0 µm
8
5.0 µm
9

Appendix:

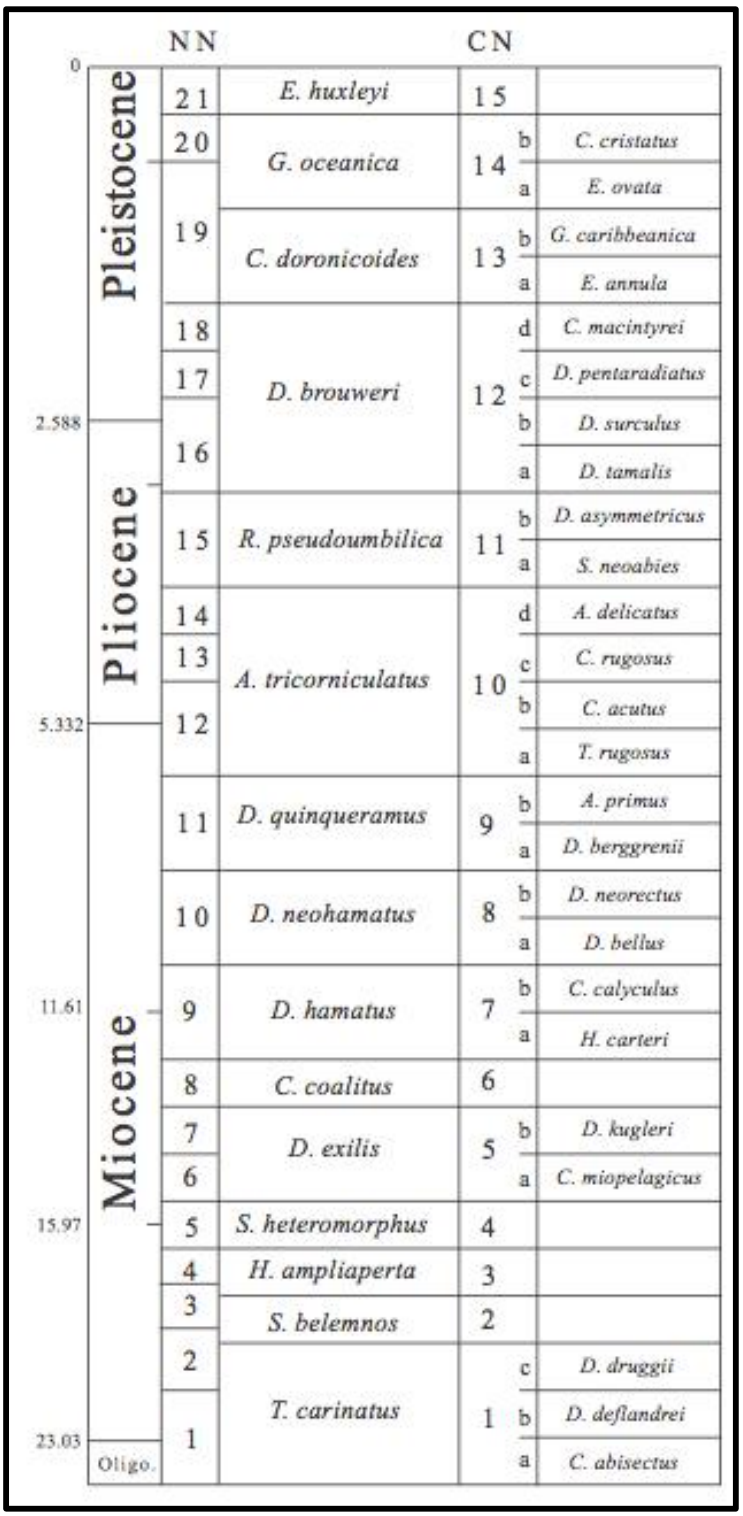

Appendix 1: Okada and Bukry (1980) zonation scheme

Foram. Zones			Calcareous Nannoplankton Zones		Datum Indicators
Quat.		N 23	NN 21	Emiliania huxleyi Zone	first E. huxleyi
			NN 20	Gephyrocapsa oceanica Zone	last P. lacunosa
		N 22	NN 19	Pseudoemilia lacunosa Zone*	last D. brouweri
Pliocene	Upper	N 21	NN 18	Discoaster brouweri Zone	last D. pentaradiatus
			NN 17	Discoaster pentaradiatus Zone	last D. surculus
		N 20	NN 16	Discoaster surculus Zone	last R. pseudoumbilica
	Lower	N 19	NN 15	Reticulofenestra pseudoumbilica Zone*	last C. tricorniculatus
			NN 14	Discoaster asymmetricus Zone*†	first D. asymmetricus
		N 19	NN 13	Ceratolithus rugosus Zone*	first C. rugosus
Miocene	Upper	N 18	NN 12	Ceratolithus tricorniculatus Zone*	last D. quinqueramus
			NN 11	Discoaster quinqueramus Zone*†	first D. quinqueramus
		N 16	NN 10	Discoaster calcaris Zone	last D. hamatus
	Middle	N 15	NN 9	Discoaster hamatus Zone	first D. hamatus
			NN 8	Catinaster coalitus Zone	first C. coalitus
			NN 7	Discoaster kugleri Zone	first D. kugleri
			NN 6	Discoaster exilis Zone	last S. heteromorphus
		N 9	NN 5	Sphenolithus heteromorphus Zone	last H. ampliaperta
		N 8	NN 4	Helicopontosphaera ampliaperta Zone	last S. belemnos
	Lower		NN 3	Sphenolithus belemnos Zone	last T. carinatus
			NN 2	Discoaster druggi Zone	first D. druggi
		N 4	NN 1	Triquetrorhabdulus carinatus Zone	last H. truncata
		N 3			

Appendix 2: Martini (1971) zonation scheme.

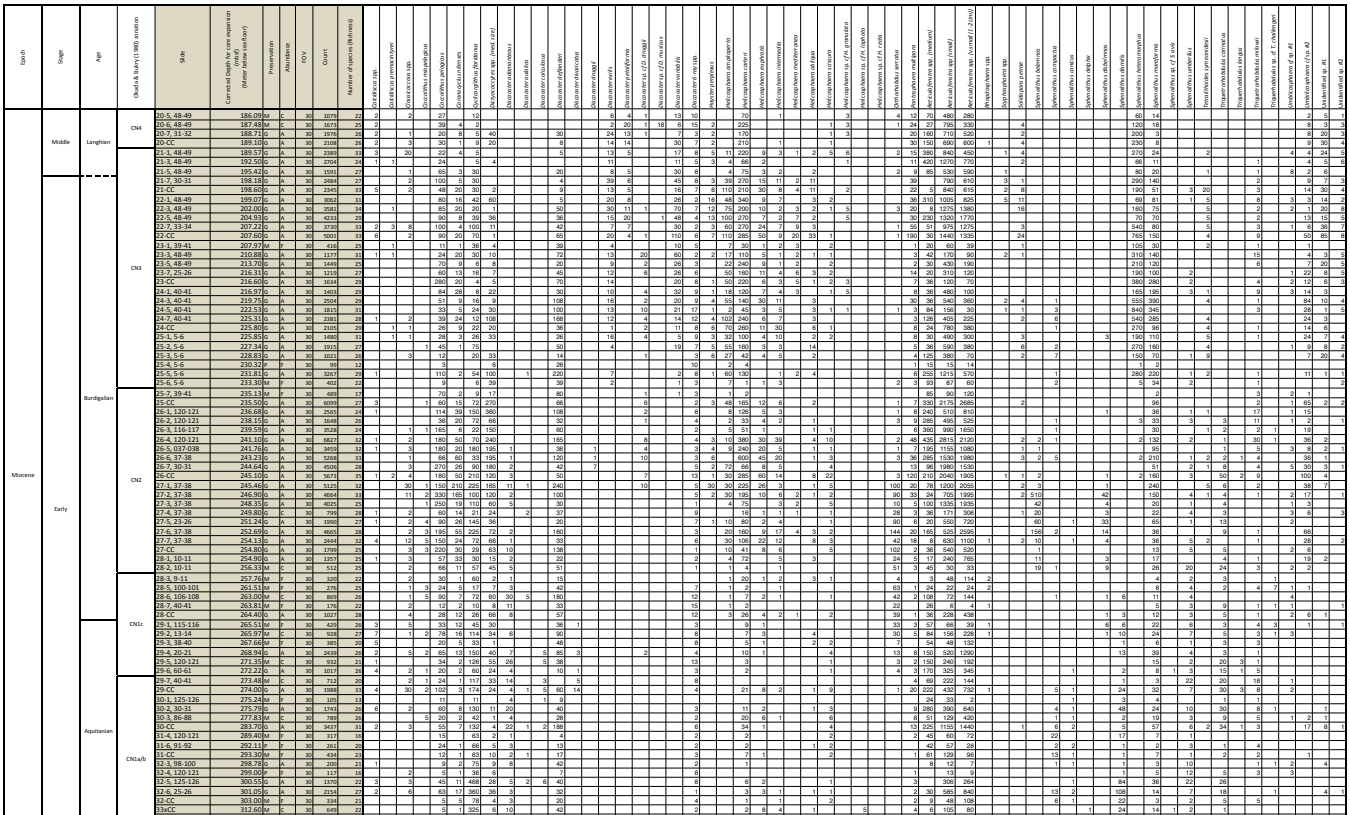

Appendix 3: Distribution chart for Hole 959A showing species counts

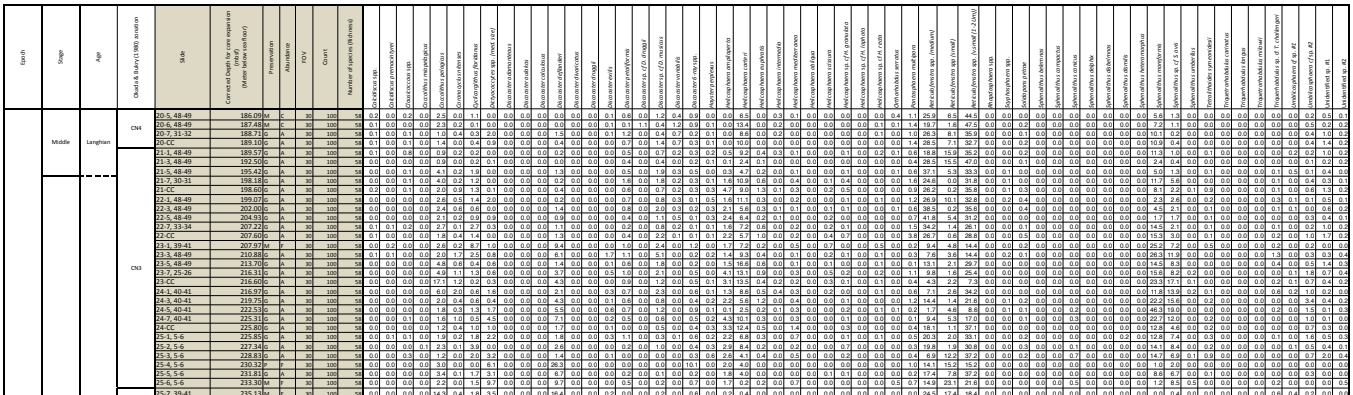

Appendix 4: Distribution chart for Hole 959A showing species percentages per sample.

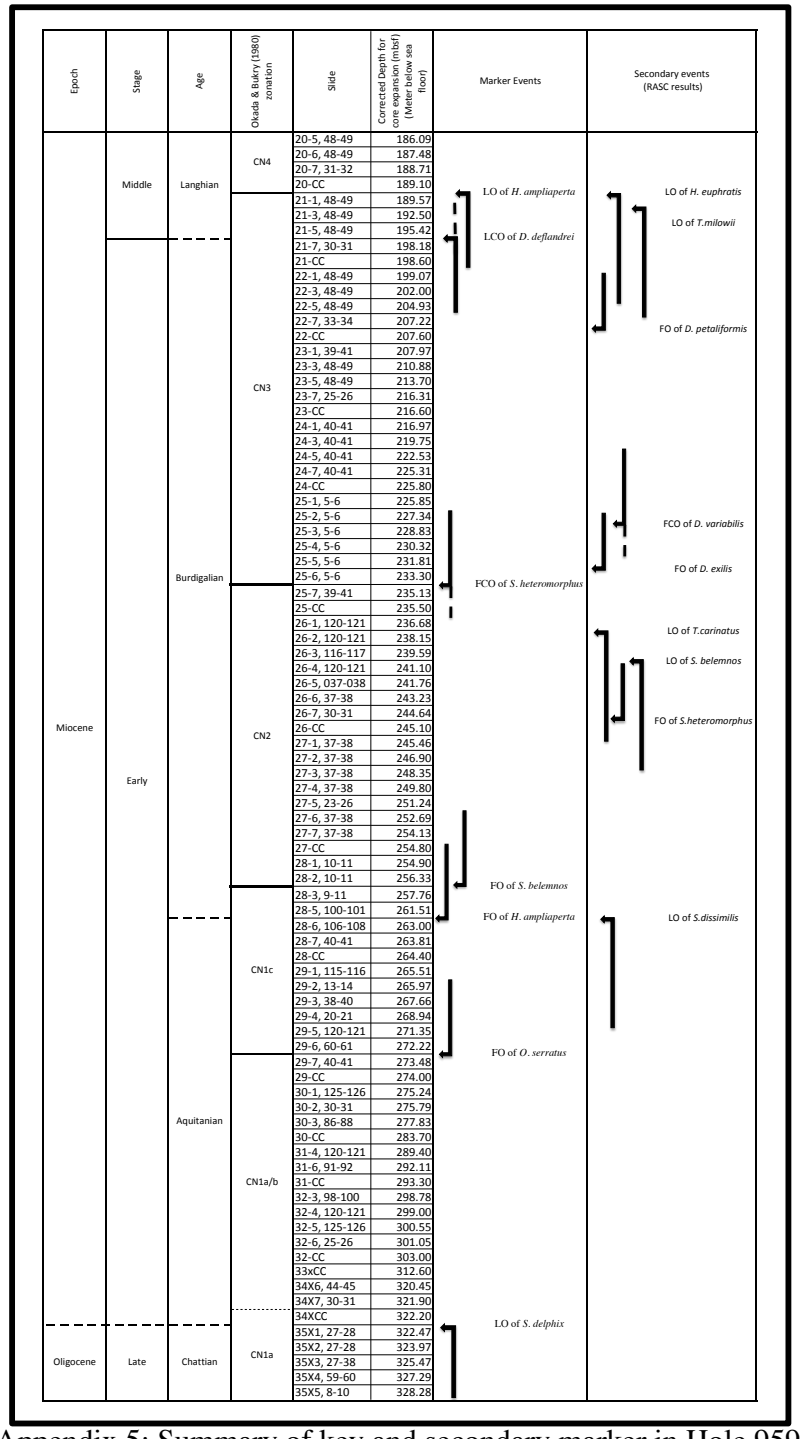

Appendix 5: Summary of key and secondary marker in Hole 959A.

Depth	Age	Error Depth	Error Age	Label
270.15	20.43	0.39		FO *Helicosphaera ampliaperta*
189.33	14.91	0.47		LO *Helicosphaera ampliaperta*
262.25	19.03	1.49		FO *Sphenolithus belemnos*
240.34	17.95	1.51		LO *Sphenolithus belemnos*
322.24	23.08	0.07	0.024	LO *Sphenolithus delphix*
322.24	22.59	0.07	0.347	FO *Sphenolithus disbelmnos*
234.22	17.72	1.83		FCO *Sphenolithus hetermorphous*
237.42	18.75	1.47	0.868	LO *Triquetrorhabdulus carinatus*
244.87	22.82	0.46		FO *Discoaster druggii*
193.96	15.80	2.92		LCO *Discoaster deflandrei*

Appendix 6: Table showing actual values used to plot Age/Depth model in OriginPro software for Hole 959A with the Error bar values for age and depth.

Site/Hole	Equation
959A	Y =0.0585X+3.9496
563	Y =0.14807X-21.66397
897C	Y =0.01051X+18.89645
898A	Y =0.07773X+3.59199
900A	Y =0.12783X-9.04359
558	Y =0.17871X-36.34122
960A	Y =0.3544X-12.66909
960C	Y =0.28493X-12.89799

Appendix 7: Equations used to interpolate age values. Equations obtained from the linear relationship of Age and Depth model for each Site/Hole.